AD/COM

Fifth Quarterly Progress Report
Task I Report

STUDY, EVALUATION AND ANALYSIS OF UNIFIED S-BAND SYSTEM FOR APOLLO GROUND NETWORK

1 July 1965 - 30 September 1965

Contract No. NAS 5-9702

by

Chi-hau Chen
Cesar A. Filippi
Kenneth W. Kruse

Prepared for

National Aeronautics and Space Administration
Goddard Space Flight Center
Greenbelt, Maryland

Approved by Steven M. Sussman
Director of Research

ADCOM, Inc.
808 Memorial Drive
Cambridge, Massachusetts

RQ7-51515

TABLE OF CONTENTS

LIST OF ILLUSTRATIONS

Chapter I

INTRODUCTION

The contents of this report constitute efforts on Task I, which is a basic evaluation and performance analysis of the Unified S-band System. The topics covered in this report are as follows:

1.1 Apollo USB Phase-Locked Frequency Demodulators

Because of the importance of phase-locked FM demodulators in the USB system, they require particular attention when system performance is discussed, especially near operating thresholds. Certain assumptions are generally made about demodulator operation and effects on noise. This section analyzes phase-locked demodulators thoroughly and determines the limitations on these assumptions. The analysis is applicable to the carrier frequency demodulator and voice subcarrier demodulator.

1.2 Acquisition Time for the Apollo Ranging Code

The acquisition time for the Apollo USB lunar length ranging code is computed including the effect of noise on the received clock. This noise will appear on the receiver generated code as well as the reference to the correlator. Curves of acquisition time vs signal-to-noise density are plotted for each of the three clock loop bandwidth positions.

1.3 Interference with the Carrier Phase-Locked Loop

A condition of possible carrier loop interference during simultaneous LEM-CSM PM operation is hypothesized. The mean-square-error for varying amounts of this interference are then calculated. The rejection required in the receiver first IF filter and second mixer are estimated on the basis of these interference calculations.

Chapter II

DISCUSSION

2.1 Apollo USB Phase-Locked Frequency Demodulators

2.1.1 Introduction

Phase-locked loops are used as frequency demodulators in several places in the Apollo Unified S-band System data demodulator. Typical of these is the carrier frequency demodulator, although the 1.25 Mc voice subcarrier demodulator has essentially the same problems to be resolved. In previous analyses the phase-locked FM demodulators have been modeled as ideal frequency discriminators, in that they have for an output the derivative of the input phase. Also, the additive white input noise has been assumed to become white phase noise. It is useful to know under which conditions these demodulators perform according to the above assumptions, and if they depart from the assumptions, what form the departure takes. To resolve these questions the phase-locked demodulator will be analyzed in some detail.

The linear phase transfer model of phase-locked loop (PLL) systems is widely used for analyzing the tracking or demodulation performance of these systems once the signal acquisition has been accomplished. The locking behavior of these systems is determined from the phase error conditions existing in the loop when tracking a given signal phase in the presence of noise. The phase error in reproducing the noise-free signal phase is usually called distortion or dynamic error, while the additional phase error due to the additive input noise is called the noise error. The latter is random in nature and is conveniently characterized by its rms value or by a peak value derived from the rms with the aid of an assigned peak factor. It is customary to assume that the additive phase noise appearing as an input in the linear model has a flat power density

spectrum independent of the signal phase, which results in the rms noise error being completely specified by the input SNR defined in the loop phase noise bandwidth established from the loop phase transfer function. We will now take a closer look at the phase noise characterization and study the conditions that validate the aforesaid approach.

2.1.2 PLL Phase Transfer Models

The block diagram of the PLL receiver is shown in Fig. 1. The input consists of the angle-modulated signal plus additive, zero-mean, stationary white noise independent of the signal. We will assume that the IF stages do not distort the signal so that the composite IF output is the sum of a constant-amplitude, angle-modulated signal plus narrowband noise, i.e.,

$$e_{if}(t) = E_s \sin[\omega_s t + \phi_s(t)] + V(t) \sin[\omega_s t + \phi_n(t)] \qquad (1)$$

where $\phi_s(t)$ is the signal phase information and $V(t)$ and $\phi_n(t)$ are the random envelope and phase of the narrowband noise representation.

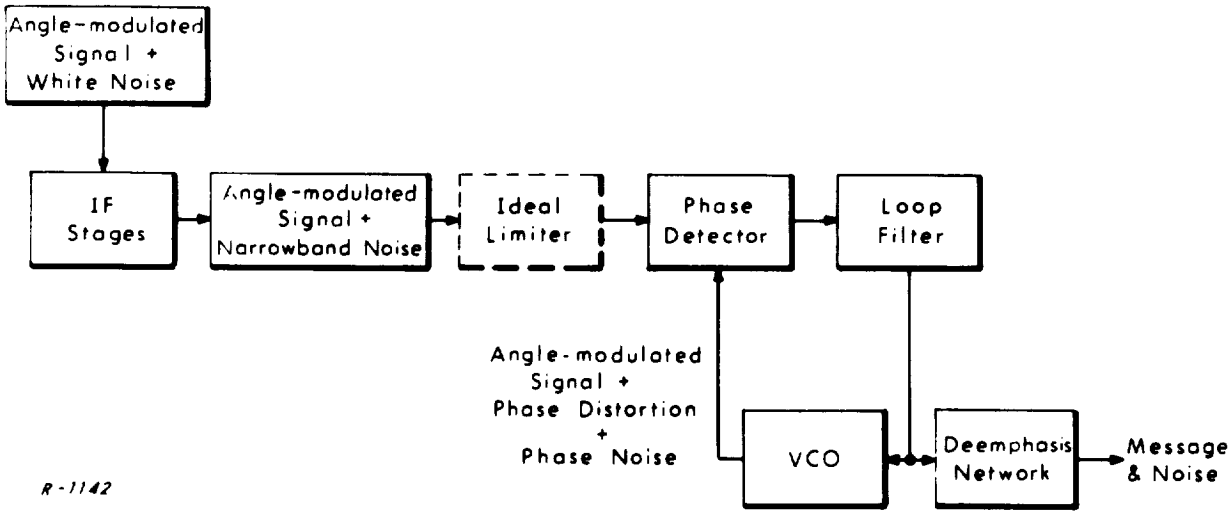

Fig. 1 Block Diagram of Carrier Frequency Demodulator.

It is convenient to rewrite the IF output as a single sinusoid in order to account for the possible presence of an (ideal) amplitude limiter preceding the PLL system:

$$e_{if}(t) = A(t)\,\sin\left[\omega_s t + \phi_s(t) + \tan^{-1}\frac{V(t)\,\sin\psi(t)}{E_s + V(t)\,\cos\psi(t)}\right] \tag{2}$$

where

$$A(t) = \begin{cases} K_\ell \text{ with a limiter} & (3a) \\ \sqrt{\left[E_s + V(t)\,\cos\psi(t)\right]^2 + \left[N(t)\,\sin\psi(t)\right]^2} \text{ without a limiter} & (3b) \end{cases}$$

and

$$\psi(t) = \phi_s(t) - \phi_n(t) \tag{4}$$

At this stage it is useful to define the random variables

$$y_c(t) = V(t)\,\cos\psi(t)\,, \quad y_q(t) = V(t)\,\sin\psi(t) \tag{5}$$

which can be found to represent the cophasal and quadrature noise components about the modulated signal phase, i.e.,

$$n(t) = y_c(t)\,\sin\left[\omega_s t + \phi_s(t)\right] + y_q(t)\,\cos\left[\omega_s t + \phi_s(t)\right] \tag{6}$$

so that the PLL input of Eq. (1) becomes

$$e_{if}(t) = A(t)\,\sin\left[\omega_s t + \phi_s(t) + \tan^{-1}\frac{y_q(t)}{E_s + y_c(t)}\right] \tag{7}$$

where

$$A(t) = \begin{cases} K_\ell \text{ with a limiter} & (8a) \\ \sqrt{[E_s + y_c(t)]^2 + y_q^2(t)} \quad \text{without a limiter} & (8b) \end{cases}$$

We will now assume that the PLL system uses a phase detector whose operation can be described as multiplying its two inputs (e. g., a sinusoidal static characteristic such as that obtained with a diode bridge or envelope detector circuit where the VCO output oscillations have an amplitude sufficiently larger than that of the PLL input oscillations). If the VCO output signal is represented by

$$e_o(t) = E_o \cos[\omega_s t + \phi_o(t)] \tag{9}$$

where $\phi_o(t)$ represents the PLL estimate of the input signal phase, then the baseband phase detector output is given (within a proportionality factor) by

$$e_d(t) = A(t) \sin\left[\phi_s(t) - \phi_o(t) + \tan^{-1} \frac{y_q(t)}{E_s + y_c(t)}\right] \tag{10a}$$

$$= E(t)\left\{\left[1 + \frac{y_c(t)}{E_s}\right] \sin\phi(t) + \frac{y_q(t)}{E_s} \cos\phi(t)\right\} \tag{10b}$$

where

$$E(t) = \begin{cases} \dfrac{K_\ell E_s}{\sqrt{[E_s + y_c(t)]^2 + y_q^2(t)}} \quad \text{with a limiter} & (11a) \\ E_s \text{ without a limiter} & (11b) \end{cases}$$

and

$$\phi(t) = \phi_s(t) - \phi_o(t) \tag{12}$$

The general phase transfer models of the PLL system are then those shown in Figs. 2 and 3 where F(p) represents the loop filter and K is the loop gain due to the phase detector and VCO sensitivities in $\sec^{-1}$.

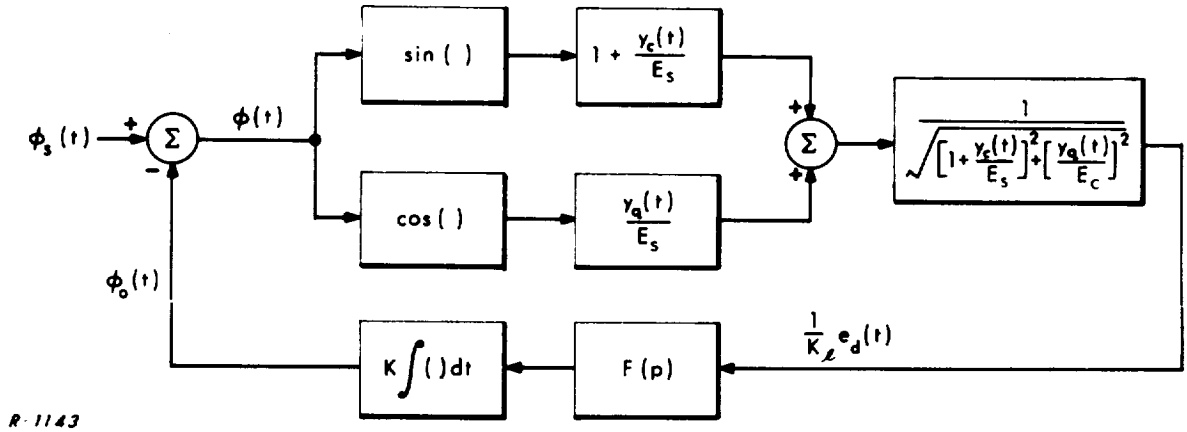

Fig. 2 Nonlinear (Time-Variant) PLL Phase Transfer Model With a Limiter.

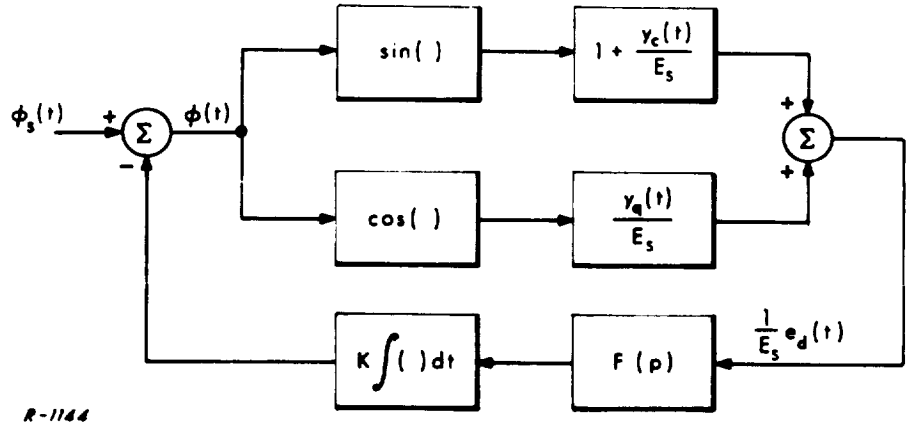

Fig. 3 Nonlinear (Time-Variant) PLL Phase Transfer Model Without a Limiter.

The PLL thus behaves as a nonlinear time-variant system in general. However, under high SNR and small phase error conditions, the cophasal noise may be neglected and the nonlinear operators may be linearized, as a first approximation. The phase detector output then becomes

$$e_d(t) = \begin{cases} K_\ell \left[\phi(t) + \dfrac{y_q(t)}{E_s} \right] & \text{with a limiter} \qquad (13a) \\ E_s \left[\phi(t) + \dfrac{y_q(t)}{E_s} \right] & \text{without a limiter} \qquad (13b) \end{cases}$$

and the corresponding linear time-invariant model of the PLL is then that shown in Fig. 4, where the equivalent phase noise input is given by

$$\psi_n(t) = \frac{y_q(t)}{E_s} \qquad (14)$$

Notice that the approximations involved in deriving the linear model are slightly different according to whether a limiter is present or not.

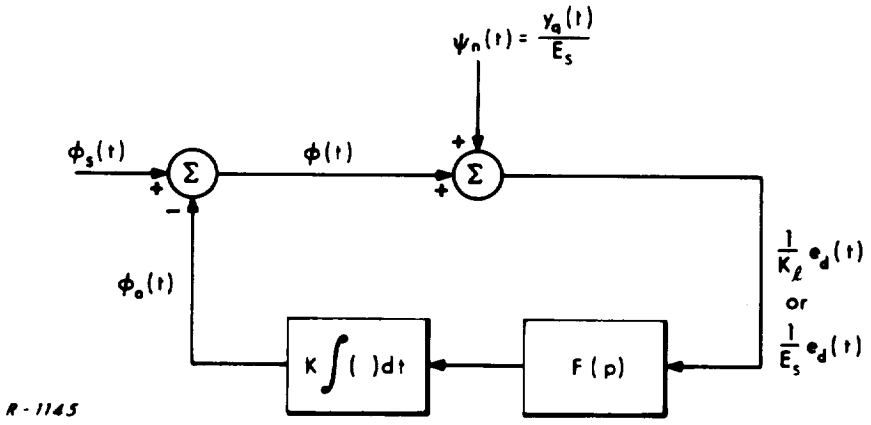

Fig. 4 Linear (Time-Invariant) PLL Phase Transfer Model.

2.1.3 Analysis of the Linear Model

The linear model of Fig. 4 defines a phase transfer function at the VCO output as

$$H_\ell(s) = \frac{KF(s)}{s+KF(s)} \tag{15}$$

and the loop phase error in estimating the signal phase $\phi_s(t)$ is given by

$$\phi(s) = \phi_s(s) - \phi_o(s) = [1 - H_\ell(s)]\,\phi_s(s) - H_\ell(s)\,\psi_n(s) \tag{16}$$

The first term is a linear phase distortion error and the second one is a phase error due to noise. The mean-square distortion error can be evaluated from the power density spectrum $S_{\phi_s}(\omega)$ of the signal phase $\phi_s(t)$ as

$$\sigma_d^2 = \int_{-\infty}^{\infty} |1 - H_\ell(j\omega)|^2 S_{\phi_s}(\omega) \frac{d\omega}{2\pi} \text{ rad}^2 \tag{17}$$

while the mean-square noise error is obtained from the power density spectrum $S_{\psi_n}(\omega)$ of $\psi_n(t)$ as

$$\sigma_n^2 = \int_{-\infty}^{\infty} |H_\ell(j\omega)|^2 S_{\psi_n}(\omega) \frac{d\omega}{2\pi} \text{ rad}^2 \tag{18}$$

While the distortion error of Eq. (17) can be directly evaluated from the signal phase spectrum $S_{\phi_s}(\omega)$, the evaluation of the noise error requires the study of the equivalent phase noise input $\psi_n(t)$ and its relation to the additive IF noise $n(t)$.

The cophasal and quadrature noise components (about the modulated signal phase) $y_c(t)$ and $y_q(t)$ of Eq. (6) can be related to the more familiar cophasal and quadrature components about the unmodulated carrier, i.e.,

$$n(t) = x_c(t) \sin\omega_s t + x_q(t) \cos\omega_s t \tag{19}$$

by the transformation

$$y_c(t) = x_c(t)\cos\phi_s(t) + x_q(t)\sin\phi_s(t) \tag{20a}$$

$$y_q(t) = x_c(t)\sin\phi_s(t) - x_q(t)\cos\phi_s(t) \tag{20b}$$

Hence, the autocorrelation function of the phase noise $\psi_n(t) = \frac{y_q(t)}{E_s}$ is given by

$$R_{\psi_n}(\tau) = \frac{1}{E_s^2} E\{y_q(t)\, y_q(t+\tau)\}$$

$$= \frac{1}{E_s^2} R_{x_q}(\tau)\, E\{\cos[\phi_s(t) - \phi_s(t+\tau)]\} + \frac{1}{E_s^2} R_{x_q x_c}(\tau)\, E\{\sin[\phi_s(t) - \phi_s(t+\tau)]\} \tag{21}$$

where $R_{x_q}(\tau) = R_{x_c}(\tau)$ is the autocorrelation function of $x_q(t)$ or $x_c(t)$, and $R_{x_q x_c}(\tau) = -R_{x_c x_q}(\tau)$ is the cross-correlation function of $x_q(t)$ and $x_c(t)$ in this order. Moreover, by noting that the joint characteristic function of $\phi_s(t)$ and $\phi_s(t+\tau)$ is defined as

$$M_{\phi_s(t)\,\phi_s(t+\tau)}(j\nu_1, j\nu_2, \tau) = E\left\{e^{j[\nu_1\phi_s(t) + \nu_2\phi_s(t+\tau)]}\right\} \tag{22}$$

then Eq. (21) can be rewritten as

$$R_{\psi_n}(\tau) = \frac{1}{E_s^2} R_{x_q}(\tau)\, \mathrm{Re}\left\{M_{\phi_s(t)\,\phi_s(t+\tau)}(j, -j, \tau)\right\}$$

$$+ \frac{1}{E_s^2} R_{x_q x_c}(\tau)\, I_m\left\{M_{\phi_s(t)\,\phi_s(t+\tau)}(j, -j, \tau)\right\} \tag{23}$$

If the signal phase process $\phi_s(t)$ is strict sense stationary, at least of order two, then the characteristic function of Eq. (22) will be independent of t and so will be the autocorrelation function of Eq. (23). Thus, the process $\psi_n(t)$ is wide sense stationary since $E\{y_q(t)\} = o$ is also satisfied, as can be verified from Eq. (20b). Moreover, if the IF is symmetric such that the power density spectrum of n(t) is even about ω_s for $\omega > o$ or if the joint characteristic function of Eq. (21) is real (e. g. , as in a gaussian process), then

$$R_{\psi_n}(\tau) = \frac{1}{E_s^2} R_{x_q}(\tau)\, \mathrm{Re}\{M_{\phi_s(t)\phi_s(t+\tau)}(j, -j, \tau)\} \tag{24}$$

and the power density spectrum $S_{\psi_n}(\omega)$ to be used in Eq. (18) is given by the convolution of the baseband replica of the IF noise power density spectrum with $E\{\cos[\phi_s(t) - \phi_s(t+\tau)]\}$. Notice that this result is valid even if $\phi_s(t)$ does not represent the actual signal but its IF-filtered version, as long as strict sense stationarity is maintained and $\phi_s(t)$ is independent of n(t). Also, notice that the distortion and noise errors are not statistically independent in general.

However, if the effective correlation time of $x_q(t)$ is small enough such that $E\{\cos[\phi_s(t) - \phi_s(t+\tau)]\} \approx 1$, as may be expected for moderately wideband modulation, then $R_{x_q}(\tau)$ may be treated as an impulse at $\tau = 0$ and Eq. (24) becomes

$$R_{\psi_n}(\tau) \approx \frac{1}{E_s^2} R_{x_q}(\tau) \approx \frac{\Phi}{E_s^2} \mu_o(\tau) \tag{25}$$

where Φ is the magnitude of the input white noise density (one-sided) in watts per cps. This approximation yields the PLL noise error from Eq. (18) in the familiar form

$$\sigma_n^2 = \frac{2\Phi}{E_s^2} \int_o^\infty |H_\ell(j\omega)|^2 \frac{d\omega}{2\pi} = \frac{2\Phi B_\ell}{E_s^2} = \frac{\Phi B_\ell}{S} \text{ rad}^2 \tag{26}$$

where $S = E_c^2/2$ is the input signal power and $B_\ell = \int_0^\infty |H_\ell(j\omega)|^2 \, d\omega/2\pi$ is the equivalent lowpass phase noise bandwidth (one-sided). An alternate bandwidth definition that incorporates a factor of 2 is the two-sided bandwidth $B_n = 2\int_0^\infty |H_\ell(j\omega)|^2 \, d\omega/2\pi = \int_{-\infty}^\infty |H_\ell(j\omega)|^2 \, d\omega/2\pi$ cps. We have chosen the former definition in order to work with lowpass functions and consider the factor of 2 as an actual increase in noise density due to folding ($\Phi \rightarrow 2\Phi$) rather than a bandwidth doubling.

A useful bound can be obtained by expanding the cosine term of Eqs. (22) and (24) in a power series and retaining the first two terms so that

$$R_{\psi_n}(\tau) \approx \frac{1}{E_s^2} R_{x_q}(\tau) \left\{1 - \left[R_{\phi_s}(o) - R_{\phi_s}(\tau)\right]\right\} \tag{27}$$

and since the receiver input noise is assumed to be white, then $R_{x_q}(\tau)$ may be evaluated as the inverse Fourier transform of the power density spectrum

$$S_{x_q}(\omega) = \Phi |\hat{H}_{\ell p}(j\omega)|^2 \tag{28}$$

where $\hat{H}_{\ell p}(s)$ is the lowpass replica of the IF bandpass filter. If the effective width of $R_{x_q}(\tau)$ is such that $R_{\phi_s}(o) - R_{\phi_s}(\tau) \ll 1$ then we can approximate Eq. (27) by

$$R_{\psi_n}(\tau) \approx \frac{1}{E_s^2} R_{x_q}(\tau) \tag{29}$$

so that

$$S_{\psi_n}(\omega) \approx \frac{\Phi}{E_s^2} |\hat{H}_{\ell p}(j\omega)|^2 \tag{30}$$

$$\sigma_n^2 \approx \frac{\Phi}{S} \int_0^\infty |H_\ell(j\omega)\, \hat{H}_{\ell p}(j\omega)|^2 \, \frac{d\omega}{2\pi} = \frac{\Phi B_{eq}}{S} \text{ rad}^2 \tag{31}$$

which defines an equivalent phase noise bandwidth B_{eq} cps that converges to B_ℓ when $\hat{H}_{\ell p}(s)$ is much wider than $H_\ell(s)$. The use of Eq. (31) with a narrow IF must be qualified since $R_{x_q}(\tau)$ will then be wide and the condition $R_{\dot{\phi}_s}(o)-R_{\dot{\phi}_s}(\tau)<< 1$ must be checked.

In summary, the evaluation of loop noise errors using Eq. (26) inherently implies a wideband IF relative to the message bandwidth occupancy, where the equivalent phase noise input into the loop may be assumed to be essentially white. When this is not the case, as when a narrow IF filter is chosen with a wider-band PLL in the carrier frequency demodulator, then this noise input is statistically dependent on the message as shown in Eq. (27), and Eq. (26) is meaningless. Notice that in this last case the sum of the mean-square noise and distortion (or dynamic) errors will not be the total mean-square phase error since these two contributions are not independent. This noise correlation considerably complicates an accurate USB FM demodulator analysis.

2.1.4 The PLL Demodulator

We will now consider the case where the VCO input signal is lowpass filtered outside the loop. The effective transfer function relating this output with the PLL phase input is given, within a proportionality factor, by

$$H(s) = s\, H_\ell(s)\, H_{\ell p}(s) \tag{32}$$

where $H_{\ell p}(s)$ is the output lowpass filter. It we assume the signal phase to be a sinusoid, i.e., $\phi_s(t) = \delta \sin \omega_m t$, then the aforesaid output signal will represent the frequency modulation $\dot{\phi}_s(t)$ as long as $H_\ell(j\omega_m) H_{\ell p}(j\omega_m) = 1$.

In turn, the corresponding output noise has a mean-square value given by

$$\overline{n_o^2(t)} = \int_{-\infty}^{\infty} \omega^2 \left| H_\ell(j\omega)\, H_{\ell p}(j\omega) \right|^2 s_{\psi_n}(\omega)\, \frac{d\omega}{2\pi} \tag{33a}$$

$$\approx \frac{\Phi}{S} \int_{o}^{\infty} \omega^2 \left| H_\ell(j\omega)\, H_{\ell p}(j\omega) \right|^2 \frac{d\omega}{2\pi} \tag{33b}$$

where the last expression corresponds to the case where Eq. (25) holds, i. e., $\hat{H}_{\ell p}(\omega)$ is much wider than $H_{\ell}(\omega)$. If this condition is not met, then Eq. (30) should be used in Eq. (33a). In the case where $H_{\ell p}(\omega)$ is much narrower than $H_{\ell}(\omega)$, then Eq. (33b) can further be approximated by

$$\overline{n_o^2(t)} \approx \frac{\Phi}{S} \int_0^{\infty} \omega^2 \left| H_{\ell p}(j\omega) \right|^2 \frac{d\omega}{2\pi} \tag{33c}$$

which matches the conventional discriminator results. However, if $H_{\ell}(\omega)$ has some overshoot at moderately low frequencies, then the parabolic noise spectrum may be emphasized by $H_{\ell}(\omega)$ prior to the lowpass filtering and some reduction in above-threshold output SNR could occur relative to a conventional discriminator, even though a threshold improvement could still exist.

We will now illustrate our comments with some experimental results involving a comparison of the output SNR capabilities of a standard FM discriminator (STD), a conventional second-order loop (PLL_2) and a third-order loop (PLL_3). The modulating signal was a sinusoid having a frequency of 1 kc and an index of 30 (wideband FM) and the IF bandpass and output lowpass filters had effective bandwidths of 100 kc and 6 kc respectively. The PLL_2 used a conventional lag network for the loop filter with breakpoints at 238 cps and 9.7 kc respectively. The ideal PLL_3 loop filter had the frequency response shown in Fig. 5 and its practical realization with nonideal differentiators only altered this response below 20 cps. The resultant output SNR vs input SNR of the three demodulators in question are shown in Fig. 6 and it is noted that the PLL_3 yields the largest threshold improvement over the STD at the expense of some small SNR degradation above threshold. This degradation is attributed to the low frequency noise emphasis introduced by the PLL_3 loop filter as a consequence of its low frequency gain.

It should be well understood that the threshold improvements illustrated in Fig. 6 are only characteristic of the wideband FM case treated. As the modulation index is reduced, the PLL threshold occurs at a higher input SNR

and the threshold improvement capabilities over the standard demodulator eventually disappear. This effect is illustrated in Fig. 7, where the two sets of curves correspond to modulation indices of 20 and 10 respectively. Since the Apollo USB FM modes utilize modulation indices of 2.0 or less, it is clear that the phase-locked demodulator can give no improvement over the conventional frequency discriminator. The voice FM link again uses a low modulation index so that here too no threshold improvement can be expected.

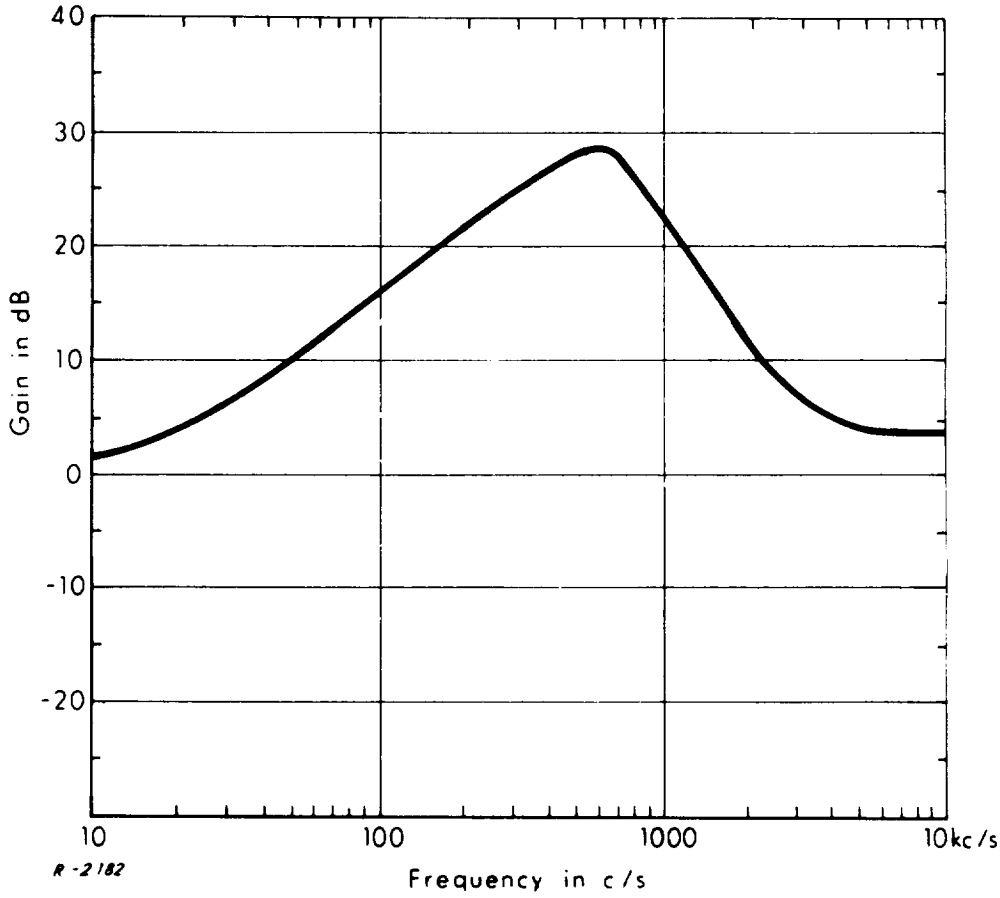

Fig. 5 Ideal Frequency Response of the PLL_3 Loop Filter.

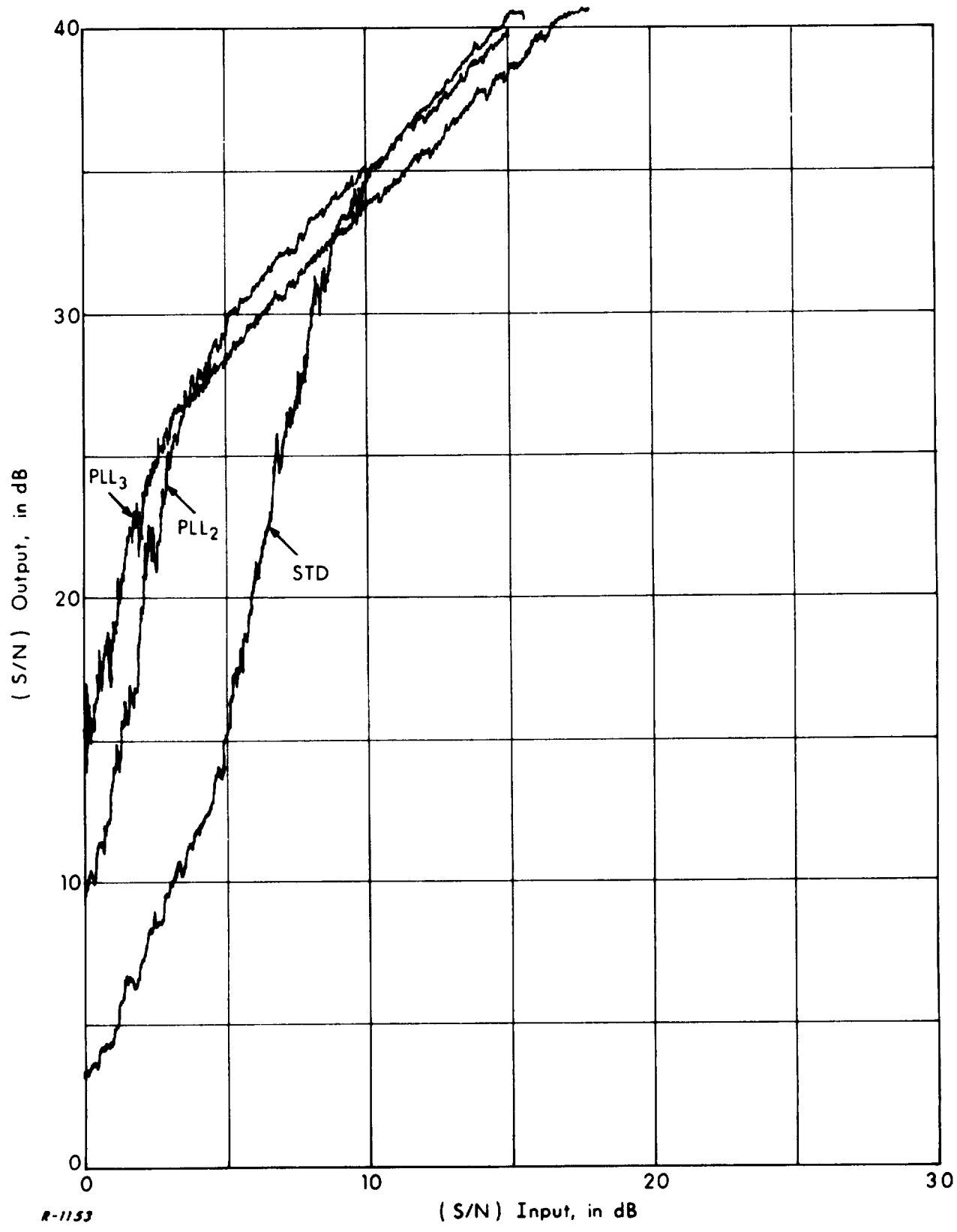

Fig. 6 Experimental Threshold Curves: modulation index = 30.

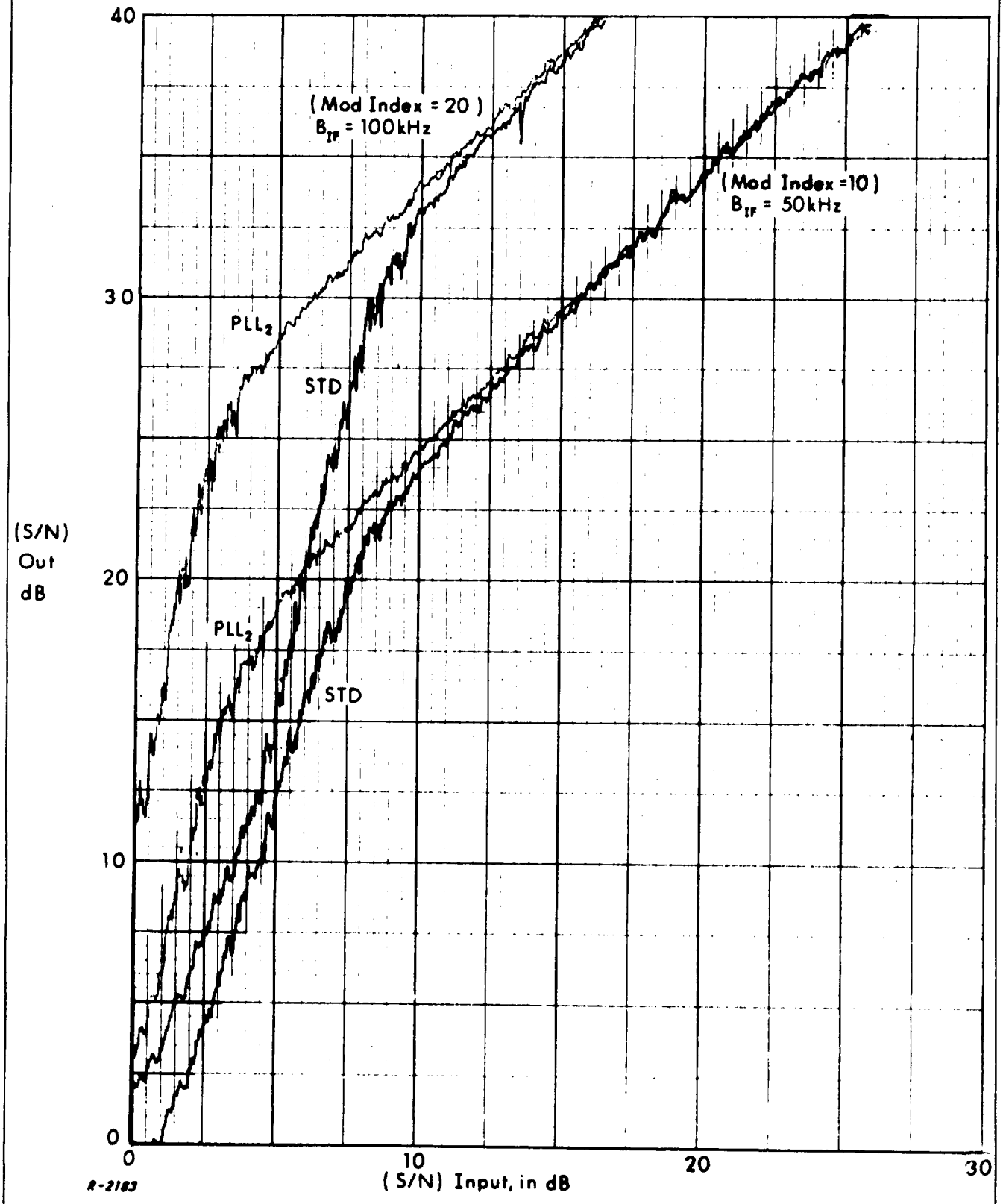

Fig. 7 Threshold Improvement vs Modulation Index ($B_{\ell p}$ = 5 kc).

2.1.5 Conclusion

The previous sections have analyzed the phase transfer behavior of the PLL system in the presence of a signal angle modulation. The phase transfer model is in general nonlinear time-variant and becomes linear time-invariant under high SNR, small phase error conditions. The equivalent phase noise input to the linear model is in general statistically dependent on the signal phase $\phi_s(t)$ and can be considered as independent when $R_{\dot{\phi}_s}(o) - R_{\dot{\phi}_s}(\Delta) \ll 1$, where Δ is the effective correlation time of the additive baseband noise at the receiver input. Under these conditions, the VCO phase noise output can be evaluated from the equivalent phase transfer function resulting from the cascade of the IF baseband transfer function and the PLL linear phase transfer function. Also, the PLL demodulator will match the conventional discriminator performance above-threshold as long as the output filter is sufficiently narrower than the loop transfer function.

2.2 Acquisition Time for the Apollo Ranging Code

2.2.1 Introduction

The word error probabilities for communication with orthogonal codes were obtained by Viterbi[1]. In many practical binary communication systems, an estimate of the phase of the received signal for bit synchronization is obtained by using a coherent tracking device such as a phase-locked loop. The bit phase reference thus obtained is noisy and the error probability will be degraded. The acquisition time-error probability relationship of a coded ranging system can be determined by using the word error probabilities derived for communication systems. The Apollo unified S-band ranging system utilizes a combination of subcodes to create the complete ranging code. Also, maximal likelihood detection is used for the acquisition of each subcode. The subcodes form "very nearly orthogonal" codes and little error is made in applying the error probability results for orthogonal codes with maximum likelihood detection in the computation of these range code acquisition results. The procedure of computing the acquisition time with a noisy clock and reference code will be described in this chapter.

2.2.2 Ranging System Model

For purposes of this analysis, the important part of the ranging equipment is the range clock receiver illustrated in Fig. 8. The received code from the sum channel receiver IF output appears as PM with 0.2 radian (currently) deviation on the 10 Mc IF carrier. A 10 Mc reference frequency which is in-phase with the carrier is biphase modulated with the locally generated code from the decoder. The two modulated 10 Mc signals are combined in the balanced detector, performing demodulation and multiplication of codes simultaneously. The received code contains a clock component which is not included in the decoder output. Thus, when the codes match, only the clock will remain at the detector output, containing the full signal power. The received code is composed of four subcodes as well as the clock and is so arranged that a clock component is available even when there is no correlation with any of the decoder subcodes. Likewise the decoder output during each of the acquisition steps will always maintain the clock output with clock level being an indication of subcode correlation. The code structures, correlation levels, and received code spectrum are discussed in detail in Chapter IV of the First and Chapter IV of the Second Quarterly Progress Reports.

The clock loop locks to the clock component at the output of the clock filter. The actual VCO arrangement involves the transmitted clock, whose frequency can be varied over a small range, and effectively tunes the VCO to the correct clock frequency. The VCO also drives the decoder through the Code Clock Transfer Loop (CCTL), which is not actually a part of the Range Clock Receiver but interfaces with it as shown. The various functions of the CCTL will not all be described here. During code acquisition the CCTL is a wideband phase-locked loop which faithfully reproduces its input, having a negligible effect on the Range Clock Receiver.

The amplitude of the clock component is detected in the correlation detector and the output goes to an A/D converter for a digital integration. The acquisition assembly performs all the control and decision functions to produce maximal likelihood ratio detection of the correct shift of each subcode.

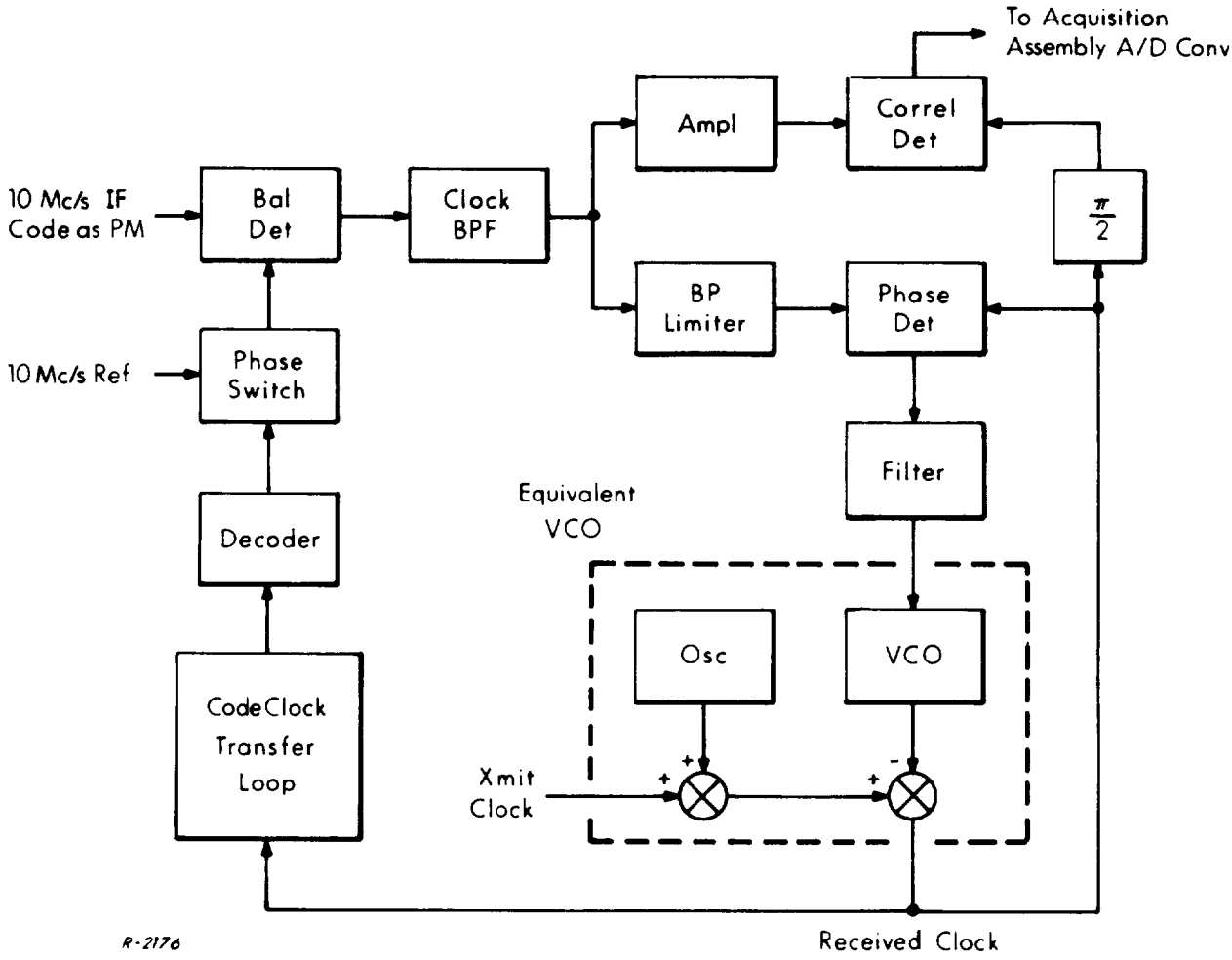

Fig. 8 Range Clock Receiver.

A more convenient model can be produced by making three simplifications to Fig. 8. This model appears in Fig. 9 and has a simple VCO in place of the actual VCO structure. The CCTL has been replaced by the $\frac{\pi}{2}$ phase shift it introduces, and at the input the RF functions have been eliminated and only the baseband code appears.

2.2.3 Error Probability Computation

The input signal is contaminated by additive white gaussian noise with power density N_o watts/cps (single-sided). The received code may be written as $\pm A_r + N_1(t)$ where $N_1(t)$ represents the input noise. The reference code, at the input to the first product detector, has the form $\pm B$ with a time jitter determined by the output of the clock loop. The product detector output contains a clock component at radian frequency ω with amplitude proportional to the correlation of the subcodes or entire code. The clock BPF output is $\frac{4}{\pi}\gamma A_r \sin \omega t + N_2(t)$ where the noise $N_2(t)$ is the product of input noise and reference code, and will still be additive, white, and gaussian if the system prior to the BPF is sufficiently wideband. γ is a correlation factor. The contribution of the reference code jitter is negligible in the BPF bandwidth if the codes are uncorrelated, and it has been omitted.

The noise $N_2(t)$ will have a phase noise component at the limiter output as $k_\ell \sin[\omega t + \psi(t)]$. This signal is tracked by the clock loop. If it is assumed that the signal-to-noise ratio is such that the linear model of the loop is applicable, then the output of the loop has the approximate form $2 \sin(\omega t + \phi(t))$ and $\phi(t) = \psi(t) \boxtimes h(t)$, where $\boxtimes$ denotes convolution and $h(t)$ is the phase impulse response of the loop. $\phi(t)$ is a gaussianly distributed random process with a zero mean and variance $\sigma_\phi^2 = \frac{N_o B_n}{2P}$. The term $P = \frac{8}{\pi^2}\gamma^2 A_r^2$ is the received clock power and B_n is the noise bandwidth (two-sided) of the clock phase-locked loop.

In the correlation detector we form the product

$$p(t) = \left[\frac{4\gamma}{\pi} A_r \sin \omega t + N_2(t)\right] \quad 2 \sin[\omega t + \phi(t)] \tag{34}$$

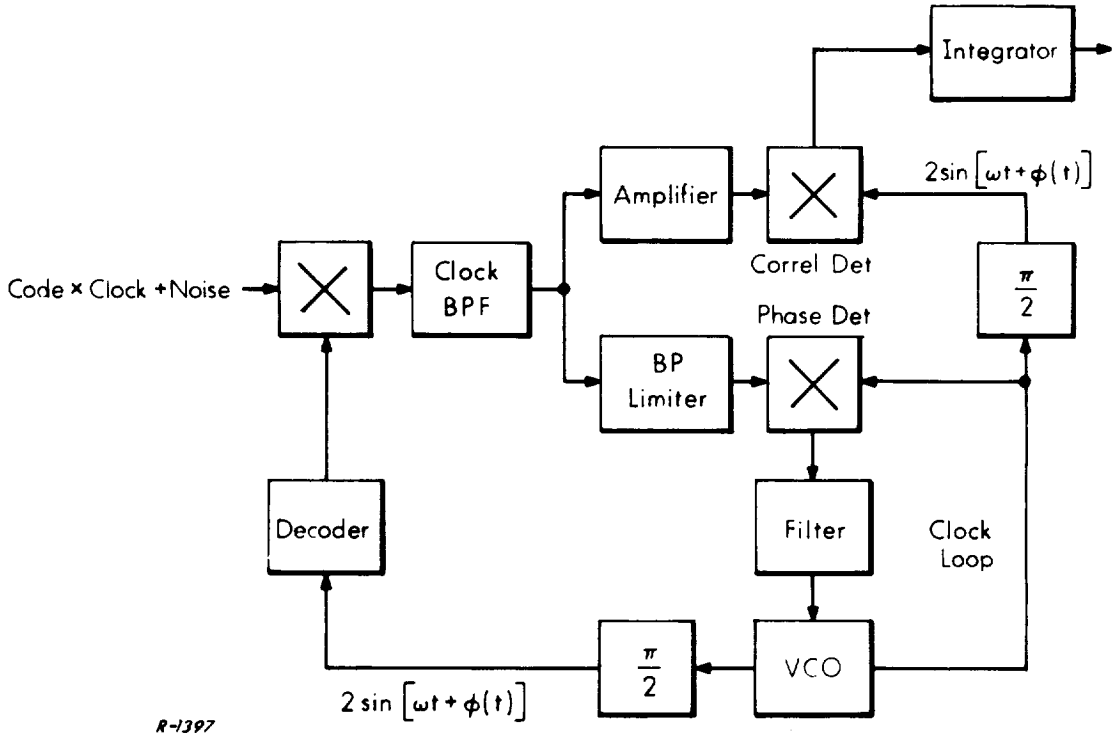

Fig. 9 Clock Receiver Model.

The second harmonic term disappears after passing through the integrator provided that ω is a multiple of $\frac{\pi}{2nT_b}$, where n is the number of information bits per word ($\log_2$ of the subcode length in code bits) and T_b is the time for receiving one information bit, or that the integration time is reasonably long. Thus, we have the output of the integrator,

$$\frac{4\gamma}{\pi} A_r \cos \phi(t) + N(t) = A \cos \phi(t) + N(t) \qquad (35)$$

where it is assumed that $\phi(t)$ is relatively constant during the T_b seconds that a bit is received. To simplify the analysis the signal output will be treated as $A \cos \phi(t)$, while in the final answer the true signal is A only. In the analysis of error probabilities we shall pretend that we have $2^n - 1$ parallel receivers each of whose decoders is set to a different code shift. Assume that the variance of the output noise of any correlator is σ^2. For a set of 2^n code words

(which approximates 2^n-1 possible code shifts), the probability that the correct one will be chosen (correct acquisition) for a given phase angle $\phi(t)$ can be written as an integral over the product of the probability densities of each correlator output

$$P(C/\phi) = \int_{-\infty}^{\infty} \frac{\exp\left[-(x-A\cos\phi(t))^2/2\sigma^2\right]}{\sqrt{2\pi}\,\sigma} \left[\int_{-\infty}^{x} \frac{e^{-(y^2/2\sigma^2)}}{\sqrt{2\pi}\,\sigma}\, dy\right]^{2^n-1} dx \qquad (36)$$

The average probability of correct decision, assuming that ϕ is gaussian with zero mean and variance σ_ϕ^2, is

$$P(C) = \int_{-\infty}^{\infty} \frac{e^{-(z^2/2\sigma_\phi^2)}}{\sqrt{2\pi}\sigma_\phi} \int_{-\infty}^{\infty} \frac{\exp\left[-(x-A\cos z)^2/2\sigma^2\right]}{\sqrt{2\pi}\sigma}\, dz \left[\int_{-\infty}^{x} \frac{e^{-(y^2/2\sigma^2)}}{\sqrt{2\pi}\sigma}\, dy\right]^{2^n-1} dx \qquad (37)$$

It is desired to obtain the average error probability as a function of signal-to-noise ratio in the clock loop. If the signal-to-noise ratio of the clock loop is sufficiently large so that $\cos z \approx 1 - \frac{1}{2}z^2$,

$$P(C) = \int_{-\infty}^{\infty} \frac{e^{-(z^2/2\sigma_\phi^2)}}{\sqrt{2\pi}\sigma_\phi} \int_{-\infty}^{\infty} e^{-\left[z^2A(x-A)+\frac{1}{4}A^2z^4\right]/2\sigma^2} dz\, \frac{e^{-(x-A)^2/2\sigma^2}}{\sqrt{2\pi}\sigma} \left[\int_{-\infty}^{x} \frac{e^{-(y^2/2\sigma^2)}}{\sqrt{2\pi}\sigma}\, dy\right]^{2^n-1} dx \qquad (38)$$

Let

$$f(z^2) = e^{-\left[z^2A(x-A)+\frac{1}{4}A^2z^4\right]/2\sigma^2}$$

Expanding $f(z^2)$ around $\overline{z^2}$ in a Taylor series, we have

$$f(z^2) = f(\overline{z^2}) + (z^2-\overline{z^2})f'(\overline{z^2}) + \frac{1}{2!}(z^2-\overline{z^2})^2 f''(\overline{z^2}) + \frac{1}{3!}(z^2-\overline{z^2})^3 f'''(\overline{z^2}) + \ldots$$

which has the expected value

$$E[f(z^2)] = f(\overline{z^2}) + (\overline{z^2})^2 f''(\overline{z^2}) + \frac{4}{3}(\overline{z^2})^3 f'''(\overline{z^2}) + \ldots\ldots$$

using the property of the gaussian distribution that $\overline{z^4} = 3(\overline{z^2})^2$ and $\overline{z^6} = 15(\overline{z^2})^3$. Substituting the derivatives

$$E[f(z^2)] = f(\overline{z^2}) \left\{ 1 + (\overline{z^2})^2 \left[-\frac{A^2}{4\sigma^2} + \frac{1}{4\sigma^4}\left(A(x-A) + \frac{1}{2}A^2\overline{z^2}\right)^2 \right] \right.$$

$$\left. + \frac{4}{3}(\overline{z^2})^3 \left[\frac{3A^2}{8\sigma^4}\left(A(x-A) + \frac{1}{2}A^2\overline{z^2}\right) - \frac{1}{8\sigma^6}\left(A(x-A) + \frac{1}{2}A^2\overline{z^2}\right)^3 \right] + \ldots \right\}$$

where $\overline{z^2} = \sigma_\phi^2 = \frac{1}{2(SNR)_{c\ell}}$ is one-half the noise-to-signal ratio of the clock loop. The expectation of the terms in the bracket with respect to x (gaussian probability distribution with mean A and variance σ^2) is

$$1 + \frac{A^4}{16\sigma^4}(\overline{z^2})^4 - \frac{A^6}{48\sigma^6}(\overline{z^2})^6 + \ldots\ldots$$

which is very close to 1 if $\overline{z^2} \leq \frac{1}{A/\sigma}$. The ratio $\frac{A}{\sigma}$ can be restricted to a minimum of around 5 to 6 for the lunar ranging code and error rate of 10^{-3}. A clock loop signal-to-noise ratio $(SNR)_{c\ell} = \frac{1}{2\overline{z^2}} \geq 3$ should allow the replacement of $E[f(z^2)]$ by $f(\overline{z^2})$. If more terms are taken in the series expansion of $\cos z$, it can be shown that the minimum $(SNR)_{c\ell}$ can be smaller and the approximation still holds. By using this approximation, the probability of correct decision can be written as

$$P(C) \approx \int_{-\infty}^{\infty} \frac{\exp -(x-A+\frac{A}{2}\sigma_\phi^2)^2/2\sigma^2}{\sqrt{2\pi}\,\sigma} \left[\int_{-\infty}^{x} \frac{e^{-(y^2/2\sigma^2)}}{\sqrt{2\pi}\,\sigma}\, dy \right]^{2^n-1} dx \qquad (39)$$

which can also be written as

$$P(C) \approx \int_{-\infty}^{\infty} \frac{e^{-(u^2/2)}}{\sqrt{2\pi}} \left[\int_{-\infty}^{u + \frac{A}{\sigma}\left[1 - \frac{1}{4(SNR)_{c\ell}}\right]} \frac{e^{-(w^2/2)}}{\sqrt{2\pi}}\, dw \right]^{2^n-1} du \qquad (40)$$

where $\frac{A}{\sigma} = \left(\frac{2nPT_b}{N_o}\right)^{1/2}$ and the clock power $P = \frac{8\gamma^2}{\pi^2} S$ where $S = A_r^2$, the total received signal power.

The probability that a word is in error (subcode has been acquired incorrectly),

$$P(E) = 1 - P(C)$$

is plotted in Fig. 10 for various values of n and signal-to-noise ratio of the clock loop as a function of energy per information bit-to-noise density ratio. The effective energy-to-noise density ratio is reduced by a factor of $\left(1 - \frac{1}{4(SNR)_{c\ell}}\right)^2$. The signal-to-noise ratio of the clock loop is related to the clock signal-to-noise density ratio by the curves shown in Fig. 11 as a function of clock loop threshold noise-bandwidth. For a given signal-to-noise density ratio of the received code, the specified error rate and the length of each subcode in bits, the required time to acquire each subcode can be obtained from Fig. 10. The integration time per information bit, T_b, is multiplied by the number of information bits in the subcode ($\log_2 p$ where the subcode is p code bits in length) to give the integration time per word, or per trial correlation. The integrations are performed sequentially so that the integration time for one trial correlation must be multiplied by the number of code bits in the subcode. Finally, the curves in Fig. 10 are based on a clock power of P/γ^2, so the integration times must be multiplied by γ^2.

As an example, for the lunar ranging code assume a code power S = -142 dBm, noise power density N_o = -174 dBm/cycle and threshold clock loop noise-bandwidth of 4 c/s. In a previous report[3], it has been established that the magnitude of the correlation output changes by 25% when a subcode is acquired, i. e., $\Delta\gamma = 1/4$. We may use $\gamma = 1/4$ if the clock SNR is correctly evaluated. From Fig. 11 the initial signal-to-noise ratio of the clock loop is obtained as 5. The required error probability is held to be constant at 10^{-3}. The subcodes have lengths p = 11, 31, 63, and 127 code bits with corresponding

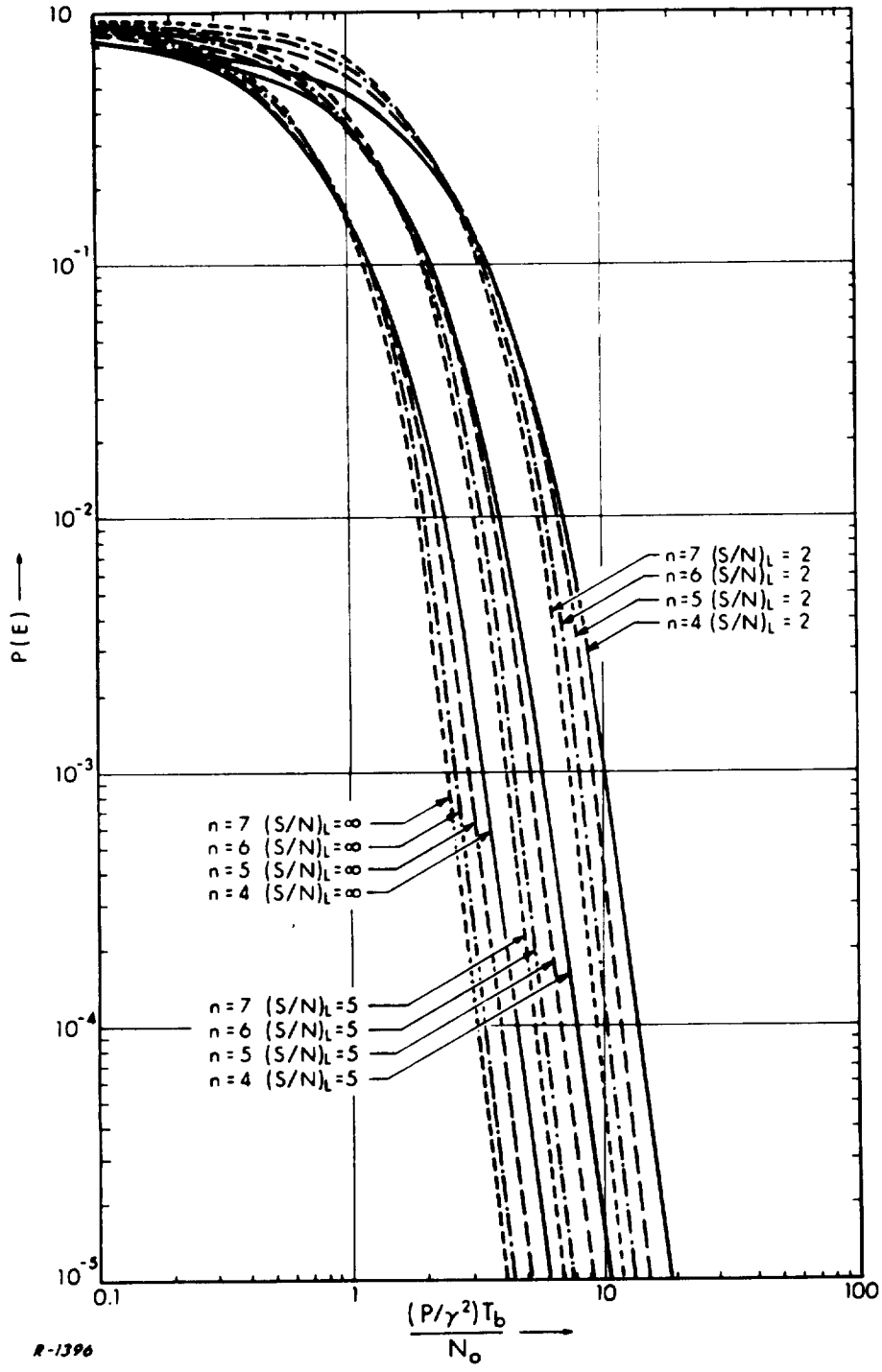

Fig. 10 Subcode Acquisition Error Probability when Clock Noise is Considered.

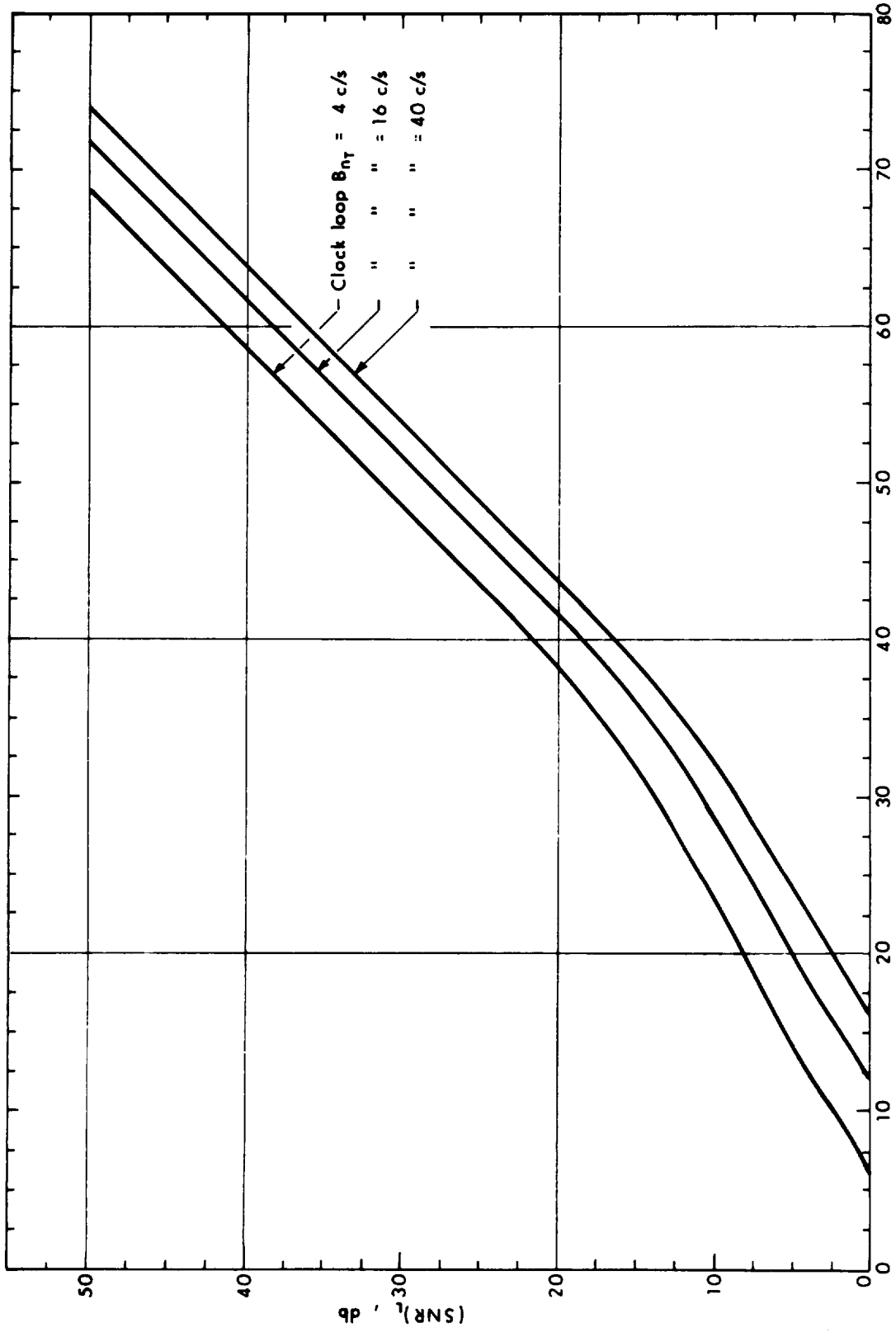

Fig. 11 Clock Loop SNR's.

values of $n = \log_2 p = 3.5$, 5, 6, and 7 information bits. The integration times per information bit may be determined from Fig. 10 as 4.60, 3.28, 3.02, and 2.74 milliseconds respectively (not yet corrected by γ^2). There are fixed delays associated with the ranging system which total 1.59 second. Then the total code acquisition time is

$$T_{aq} = \frac{1}{\gamma^2} \sum_{i=1}^{4} p_i n_i T_{b_i} + 1.59 = 69.0 \text{ sec.}$$

A plot of total acquisition time (seconds) vs code power-to-noise density ratio (dB·cps) is shown in Fig. 12 for the three clock loop threshold bandwidths: $Bn_T = 4$, 16, and 40 c/s.

2.2.4 Alternate Analysis

If the integration time may not be exactly the same as the time for receiving an information bit, a more general analysis is desirable. Only the low-frequency component at the output of the integrator will be considered, as the integrator functions as a lowpass filtering device. Thus, the output of the correlator is

$$q(\tau) = \frac{1}{\tau} \int_0^{\tau} A \cos \phi(t)\, dt \qquad (41)$$

plus an additive noise term, which is assumed to be uncorrelated with $q(\tau)$. τ is the integration time.

As $\phi(t)$ is usually small for the loop signal-to-noise ratio of interest, we have approximately, $\cos \phi(t) \approx 1 - \frac{1}{2}\phi^2(t)$, whose autocorrelation function is

$$E[(1-\tfrac{1}{2}\phi^2(t_1))(1-\tfrac{1}{2}\phi^2(t_2))] = 1 - E[\phi^2(t)] + \frac{1}{4} E[(\phi(t_1)\,\phi(t_2))^2] \qquad (42)$$

The variance of $q(\tau)$ can be written, using the expansion for $\cos \phi(t)$, as

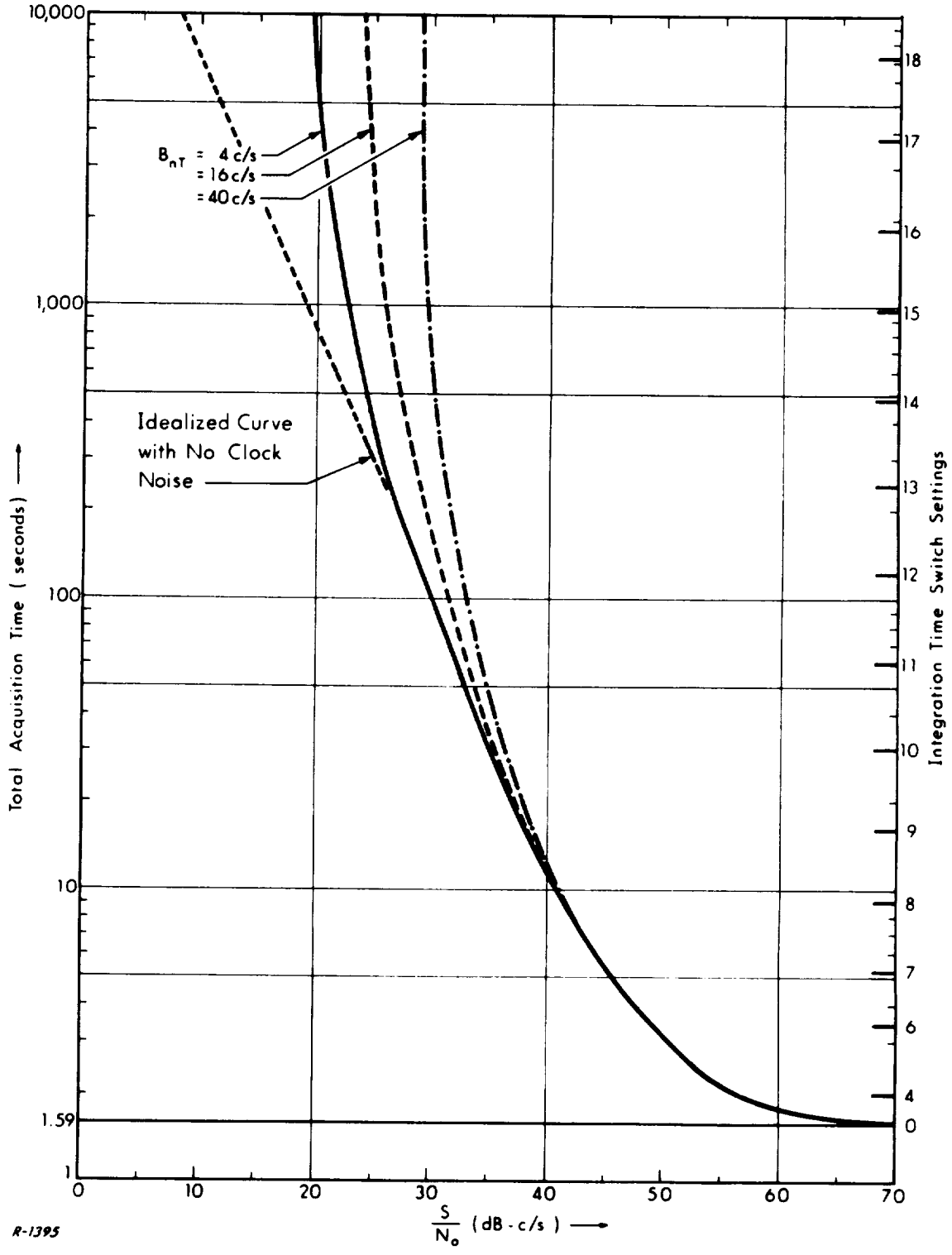

Fig. 12 Acquisition Time of the Lunar Length Code.

$$\sigma_q^2 = \frac{1}{4}\frac{A^2}{\tau^2} E\left(\left[\int_0^\tau (\phi^2(t) - E(\phi^2(t))\, dt\right]^2\right) = \frac{1}{4}\frac{A^2}{\tau^2}\int_0^\tau\int_0^\tau [R_{\phi^2}(t_1 - t_2) - R_\phi^2(o)]\, dt_1 dt_2$$

$$= \frac{1}{2}\frac{A^2}{\tau^2}\int_0^\tau (\tau - t)\,[R_{\phi^2}(t) - R_\phi^2(o)]\, dt \qquad (43)$$

where[2]

$$R_{\phi^2}(t) = R_\phi^2(o) + 2R_\phi^2(t)$$

Thus, the variance of $q(\tau)$ is

$$\sigma_q^2 = \frac{1}{2}\frac{A^2}{\tau^2}\int_0^\tau (\tau - t)\int_0^\infty G_{\phi^2}(f)\cos\omega t\, df\, dt = \frac{1}{2}\frac{A^2}{\tau^2}\int_0^\infty G_{\phi^2}(f)\left[\frac{1-\cos\omega\tau}{\omega^2}\right] df$$

$$= \frac{A^2}{\tau^2}\frac{1}{2\pi j}\int_{-j\infty}^{j\infty}\frac{1}{2\pi j}\int_{-j\infty}^{j\infty} G_\phi(S')\,G_\phi(S-S')\, dS'\left[\frac{1-\cos\tau S}{S^2}\right] dS \qquad (44)$$

To compute $G_\phi(S)$, we note that the autocorrelation function $R_\phi(\lambda)$ is given by

$$R_\phi(\lambda) = E[(\psi(u) \otimes h(u))\,(\psi(\nu) \otimes h(\nu))]$$

$$= \int_0^\infty\int_0^\infty E[\psi(u-t_1)\,\psi(u-t_2)]\, h(t_1)\, h(t_2)\, dt_1 dt_2$$

and thus

$$G_\phi(S) = |H(S)|^2\, G_\psi(S) = |H(S)|^2\,\frac{N_o}{2P} \qquad (45)$$

If a perfect clock reference is used, the variance at the output of the correlator can easily be shown as $\frac{N_o}{2\tau}$. The additional variance at the

output of the correlator due to the noisy clock depends on the tracking loop used and is given by

$$\frac{1}{2\pi j}\int_{-j\infty}^{j\infty}\frac{A^2}{\tau^2}\,\frac{1}{2\pi j}\int_{-j\infty}^{j\infty}H^2(S')\,H^2(S'-S)\left(\frac{N_o}{2P}\right)^2 dS'\left[\frac{1-\cos\tau S}{S^2}\right]dS \qquad (46)$$

If we assume that $H^2(S)$ has magnitude of unity over $-j\frac{B_n}{2}\le S\le j\frac{B_n}{2}$ and zero elsewhere, then the convolution integral,

$$\frac{1}{2\pi j}\int_{-j\infty}^{j\infty}H^2(S')\,H^2(S'-S)\,dS' = B_n - |S| \qquad -jB_n\le S\le jB_n$$
$$= 0 \qquad \text{elsewhere}$$

To evaluate Eq. (46), we further assume that $B_n\tau > 2\pi$ and that the majority of the area $\frac{1}{2\pi j}\int_{-j\infty}^{j\infty}\left[\frac{1-\cos\tau S}{S^2}\right]dS = \frac{\tau}{2}$ is in the region $-jB_n\le S\le jB_n$.

We also note that $P = A^2$. Under such conditions, Eq. (46) can be approximated fairly well by $\frac{N_o}{4\tau}\left(\frac{N_oB_n}{2P}\right)$.

The overall variance normalized by the input code power is therefore

$$\frac{1}{A_r^2}\left[\frac{N_o}{2\tau}+\frac{N_o}{4\tau}\,\frac{1}{(SNR)_{c\ell}}\right] = \frac{N_o}{2\tau A_r^2}\left[1+\frac{1}{2(SNR)_{c\ell}}\right] \approx \frac{N_o}{2\tau A_r^2\left(1-\frac{1}{4(SNR)_{c\ell}}\right)^2} \qquad (47)$$

by using the binomial expansion.

This result agrees with that of Section 2.2.3 in which the effective energy-to-noise density ratio is reduced by a factor of $\left(1-\frac{1}{4(SNR)_{c\ell}}\right)^2$ for sufficiently large clock loop signal-to-noise ratios.

2.3 Interference with the Phase-Locked Carrier Loop

2.3.1 Introduction

Several types of interference can occur in an MSFN PM receiver when LEM and CSM are being received simultaneously and both are operating in PM modes.

High-order modulation sidebands from one RF signal can overlap first-order sidebands or the carrier of the other RF signal. These sidebands occur at all multiples and sums and differences of multiples of the modulation frequencies. Fortunately the amplitudes of these components decrease rapidly as their order increases. If doppler shifts on the LEM and CSM signals are nearly the same the only overlap of frequency components will occur with third- and fourth-order voice sidebands. Telemetry sidebands will not overlap any important regions, while the ranging sidebands will not cause significant interference and will be ignored.

To illustrate the voice sideband interference, the LEM and CSM PM downlink carrier frequencies are separated by 5 Mc. The voice subcarrier has a frequency of 1.25 Mc, whose fourth harmonic is 5 Mc, so that the LEM upper fourth-order voice sideband will fall on the CSM carrier and the CSM lower fourth-order voice sideband will fall on the LEM carrier. Similarly each signal's third-order voice sidebands will fall on the other's first-order voice sidebands. The relative amplitudes of desired signal and interference can be determined assuming any difference in received RF signal powers is known and the phase deviations of the modulation on the carrier are known. Assuming a peak voice deviation of 0.7 radian and a peak telemetry deviation of 1.3 radian the sideband levels relative to the carrier can be computed. Thus for the voice sidebands

$$\frac{\text{first-order voice sideband}}{\text{carrier}} = \frac{J_1(0.7)}{J_o(0.7)} \text{ or } -8.55 \text{ dB}$$

second-order	-23.51	dB
third-order	-42.1	dB
fourth-order	-63	dB
fifth-order	-87	dB

and for the telemetry

$$\frac{\text{first-order telemetry sideband}}{\text{carrier}} = \frac{J_1(1.3)}{J_o(1.3)} \text{ or } -1.50 \text{ dB}$$

fifth-order	-57	dB

If the two RF signals are of equal strength the voice interference-to-carrier (I/C) ratio will be -63 dB if there is no voice modulation on the voice subcarrier, and much less when modulation is present because the modulated subcarrier occupies a bandwidth of either 20 kc or 35 kc while the carrier loop bandwidth is much narrower so that most of this interference will be filtered out. For unequal signal strengths the I/C ratio will be altered by the difference in levels, so that for a difference in received signals of 30 dB the weaker will suffer an I/C ratio of -33 dB. This interference is not excessive and when voice modulation spreads the frequency spectrum of the subcarrier, this source of interference can be neglected.

For equal strength signals the third-order voice interference-to-voice (I/V) ratio will be -33.5 dB. This is interference to one first-order voice sideband. The other first-order voice sideband will see virtually no interference (actually there is a fifth-order voice interference at -78.5 dB) so that the folding of voice sidebands during carrier demodulation will reduce the effective I/V ratio by 6 dB to -39.5 dB. The limiter at the input of the voice subcarrier demodulator will reduce this ratio up to 6 dB more. Here it would require a difference in levels of 30 dB or greater to cause noticeable voice interference.

With different doppler shifts on the two RF signals one possible telemetry interference must be noted. The fifth-order telemetry sideband

falls 120 kc from the other RF carrier and certain doppler conditions could make them overlap. However, the resultant I/C ratio for equal RF levels is -57 dB which is only slightly stronger than the voice interference previously discussed, and the same arguments apply to reject this as a serious mode of interference.

As a more subtle type of interference, a case of direct interference in the carrier loop will be hypothesized. The LEM and CSM PM downlink frequencies are separated by 5 Mc. If two carriers separated by 5 Mc appear at the input to the second mixer in the MSFN receiver (50 Mc converted to 10 Mc), one of the possible outputs is the 5 Mc difference frequency and another is its second harmonic, which falls at 10 Mc. This component, if sufficiently large, can cause direct interference with the desired signal. The problem would probably be worst during acquisition, although the phase errors after acquisition might also cause trouble. It is this second effect which is analyzed in the following sections.

It is well-known that, in the absence of undesired interference signals, near optimum performance of a second-order phase-locked loop (PLL) over a wide range of input signal and noise levels is possible if a bandpass limiter is used in front of the loop.[4, 5] The loop performance and the conditions for the loop to stay in lock have been investigated.[6] With the presence of interference, it is necessary that the PLL will stay in lock and perform adequate tracking of the desired signal instead of the interference. The performance of the PLL, measured as the mean-square error between the signal input and loop VCO output, is examined in this section. This error is related to the condition for the loop to stay in lock. It is assumed that the loop is adequately described by a linear phase transfer model before it loses lock. Figure 13 illustrates the schematic

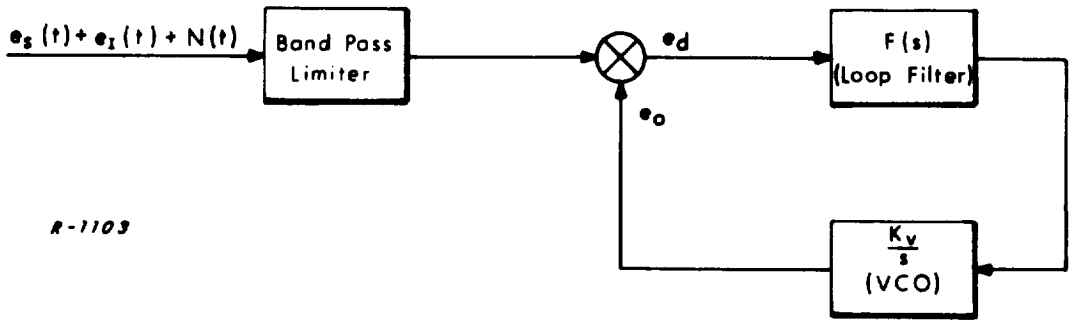

Fig. 13 Simplified PM Receiver.

diagram under consideration where $e_S(t)$, $e_I(t)$ and $N(t)$ denote signal, interference and noise at the bandpass limiter input. In Sec. 2.3.2, an estimate of the upper bound of the mean-square error is derived and the conditions for the loop to remain in lock are then obtained. For large input signal-to-noise ratios, $(S/N)_i \geq 20$ dB say, such mean-square error can be computed analytically. For smaller input signal-to-noise ratios a graphical solution is necessary. The root mean-square phase error estimate is plotted as a function of input signal-to-noise ratio for various input interference-to-signal power ratios. In Sec. 2.3.3 the effect of signal suppression is discussed.

2.3.2 System Performance Analysis

Let the input signal, interference and VCO output be denoted respectively by

$$e_S(t) = \sqrt{2S_S} \sin(\omega_S t + \phi_S(t)) \tag{48a}$$

$$e_I(t) = \sqrt{2S_I} \sin(\omega_I t + \phi_I(t)) \tag{48b}$$

$$e_o(t) = \sqrt{2} \cos(\omega t + \phi_o(t)) \tag{48c}$$

where S_S and S_I are input signal and interference powers respectively. The noise $N(t)$ is assumed to be narrowband white gaussian with power N at the bandpass limiter (BPL) input. The subscript o will be used to denote the BPL output quantities. $a^2 = S_I/S_S$ is the ratio of input interference-to-signal power. S_{SI} and S_{IS} are intermodulation terms of frequencies $2\omega_S - \omega_I$ and $2\omega_I - \omega_S$, respectively.

The loop is assumed to be initially locked to the desired signal and the interference is allowed to come within the pull-in range of the loop; thus $\omega_S \approx \omega_I \approx \omega$. The power out of the bandpass filter with center frequency ω, which follows the limiter, is equal to the power of the first harmonic in a Fourier series expansion of a rectangular waveform which has its peak-to-peak amplitude determined by the limiter (i.e., 2). Thus,the power in the first zone of the output is $8/\pi^2$. Phase expressions prove far too cumbersome to be useful. Therefore, the analysis will be conducted in the time domain. If the input of the BPL is written as

$$e_{in}(t) = \sqrt{2S_S}\ \sin\left[\omega t + \phi_S(t)\right] + a\sqrt{2S_S}\ \sin\left[\omega t + \phi_I(t)\right] + N(t) \qquad (49)$$

then the output of the BPL consists of the following significant terms

$$\frac{4\gamma}{\pi}\left\{\sin\left[\omega t + \phi_S(t)\right] + \sqrt{(S_I/S_S)_o}\ \sin\left[\omega t + \phi_I(t)\right] + \sqrt{(S_{SI}/S_S)_o}\ \sin\left[\omega t + 2\phi_S(t) - \phi_I(t)\right]\right.$$

$$\left. + \sqrt{(S_{IS}/S_S)_o}\ \sin\left[\omega t - \phi_S(t) + 2\phi_I(t)\right]\right\} + N_o(t)\sin\omega t \qquad (50)$$

where γ^2 is the fraction of signal power in the total limiter output. The initial factor

$$\frac{4\gamma}{\pi} = \sqrt{2S_{S_o}}$$

For notational convenience, let

$$\sqrt{(S_I/S_S)_o} = f, \quad \sqrt{(S_{SI}/S_S)_o} = g, \quad \sqrt{(S_{IS}/S_S)_o} = h$$

where f, g, h are functions of signal-to-noise ratio as well as interference-to-signal power ratio at the BPL input. Also, let

$$\phi_S(t) - \phi_o(t) = \phi_{e_S}(t)$$

$$\phi_I(t) - \phi_o(t) = [\phi_S(t) - \phi_o(t)] + [\phi_I(t) - \phi_S(t)] = \phi_{e_S}(t) + \phi_u(t)$$

Assume $\phi_{e_S}(t)$ to be small such that $\sin \phi_{e_S}(t) \approx \phi_{e_S}(t)$, $\cos \phi_{e_S}(t) \approx 1$. The output of the phase detector, neglecting the second harmonic terms, can be written as

$$e_d(t) \approx \frac{4\gamma}{\pi\sqrt{2}} \left\{ \sin \phi_{e_S}(t) + f \sin [\phi_{e_S}(t) + \phi_u(t)] + g \sin [\phi_{e_S}(t) - \phi_u(t)] \right.$$

$$\left. + h \sin [2\phi_u(t) + \phi_{e_S}(t)] \right\} - \frac{N_o(t)}{\sqrt{2}} \sin \phi_o(t) \qquad (51)$$

$$\approx \frac{4\gamma}{\pi\sqrt{2}} \left\{ \phi_{e_S}(t) [1 + (f+g) \cos \phi_u(t) + h \cos 2\phi_u(t)] + (f-g) \sin \phi_u(t) \right.$$

$$\left. + h \sin 2\phi_u(t) \right\} - \frac{N_o(t)}{\sqrt{2}} \sin \phi_o(t)$$

The values of the coefficients are such that $h \cos 2\phi_u(t) \ll (f+g) \cos \phi_u(t)$; thus

$$e_d(t) \approx \frac{4\gamma}{\pi\sqrt{2}} [1 + (f+g) \cos \phi_u(t)] \left\{ \phi_{e_S}(t) + \frac{f-g}{1 + (f+g) \cos \phi_u(t)} \sin \phi_u(t) \right.$$

$$\left. + \frac{h}{1 + (f+g) \cos \phi_u(t)} \sin 2\phi_u(t) \right\} - N_o'(t) \sin \phi_o(t) \qquad (52)$$

By observing Figs. 2, 3 and 4 of Ref. 4, we note that $f+g \leq 1$ except when $a \rightarrow 1$, $(S/N)_i \rightarrow \infty$. Also $|\cos \phi_u(t)| \leq 1$, so the following expansion is appropriate

$$\frac{1}{1 + (f+g) \cos \phi_u(t)} \simeq 1 - (f+g) \cos \phi_u(t) + (f+g)^2 \cos^2 \phi_u(t)$$

Thus,

$$e_d(t) \approx \frac{4\gamma}{\pi\sqrt{2}}[1 + (f+g)\cos\phi_u(t)]\left\{\phi_{e_S}(t) + [f - g - \frac{1}{2}h(f+g) + \frac{1}{4}(f+g)(f^2 - g^2)]\sin\phi_u(t) + [h - \frac{1}{2}(f^2 - g^2) + \frac{1}{2}h(f+g)^2]\sin 2\phi_u(t) + [\frac{1}{4}(f+g)(f^2 - g^2) - \frac{1}{2}h(f+g)]\sin 3\phi_u(t) + \frac{1}{4}h(f+g)^2 \sin 4\phi_u(t)\right\} - N_o'(t)\sin\phi_o(t) \quad (53)$$

We can consider the factor $\gamma[1+(f+g)\cos\phi_u(t)]$ as a phase detector gain, so that the equivalent phase transfer model of the loop has a constant-plus-time-varying gain. Consider the case of both the signal and interference having constant doppler shift upon them. As a first-order approximation, we have $\phi_u(t) = \Omega(t)$. The time-varying part of the gain will have an effect which decreases as its frequency falls outside the passband of the loop transfer function. Thus, although the gain variation is an amplitude rather than a phase variation, its contribution to interference can be approximated in the following way. Let the equivalent phase transfer model be considered as a superposition of two phase transfer models with the same closed loop transfer function H(s) as determined by the gain $K\gamma$ with the second transfer function magnitude scaled by (f+g). The time-varying gain has been replaced by a constant gain with all phase quantities multiplied by cos Ωt.

The mean-square error due to interference can be written as

$$\overline{\epsilon_u^2} = \frac{1}{2\pi j}\int_{-j\infty}^{j\infty} |H(s)|^2 \Phi_u(s)\, ds \quad (54)$$

where $\Phi_u(s)$ is the power spectral density of the undesired inputs (sin Ωt, sin $2\Omega t$, etc., terms). Thus, $\Phi_u(s)$ consists of pairs of impulse functions

located at $\omega = \pm \Omega, \pm 2\Omega, \pm 3\Omega$, etc. If we multiply the transfer function H(s) by (f+g) and denote the new transfer function by H'(s), the mean-square error due to interference, to a good approximation, is given by

$$\begin{aligned}\overline{\epsilon_u^2} = {} & \frac{1}{2}\left[(f-g) - \frac{1}{2}h(f+g) + \frac{1}{4}(f+g)(f^2-g^2)\right]^2 |H(j\Omega)|^2 \\ & + \frac{1}{2}\left[h - \frac{1}{2}(f^2-g^2) + \frac{1}{2}h(f+g)^2\right]^2 |H(j2\Omega)|^2 \\ & + \frac{1}{2}\left[-\frac{1}{2}h(f+g) + \frac{1}{4}(f+g)(f^2-g^2)\right]^2 |H(j3\Omega)|^2 \\ & + \frac{1}{8}\left[h - \frac{1}{2}(f^2-g^2) + \frac{1}{2}h(f+g)^2\right]^2 |H'(j\Omega)|^2 \\ & + \frac{1}{8}\left[(f-g) - h(f+g) + \frac{1}{2}(f+g)(f^2-g^2)\right]^2 |H'(j2\Omega)|^2 \\ & + \frac{1}{8}\left[h - \frac{1}{2}(f^2-g^2) + \frac{1}{2}h(f+g)^2\right]^2 |H'(j3\Omega)|^2 \end{aligned} \tag{55}$$

which can be computed for any specified frequency offset Ω. For a second-order loop, the damping ratio is usually in the range of 0.5 to 1.5 and $|H(s)| \leq \sqrt{2}$, $|H'(s)| \leq (f+g)\sqrt{2}$ holds. An upper bound of the estimate of root mean-square error can be written as

$$\begin{aligned}\hat{\epsilon}_u = \Big\{ & \left[(f-g) - \frac{1}{2}h(f+g) + \frac{1}{4}(f+g)(f^2-g^2)\right]^2 + \left[1 + \frac{1}{2}(f+g)^2\right]\left[h - \frac{1}{2}(f^2-g^2) + \frac{1}{2}h(f+g)^2\right]^2 \\ & + \frac{1}{4}\left[h(f+g) - \frac{1}{2}(f+g)(f^2-g^2)\right]^2 + \frac{1}{4}(f+g)^2\left[(f-g) - h(f+g)\right. \\ & \left. + \frac{1}{2}(f+g)(f^2-g^2)\right]^2\Big\}^{1/2} \end{aligned} \tag{56}$$

We will compute the root mean-square error for large input signal-to-noise ratio as well as medium input signal-to-noise ratio. Before doing this, the condition for the loop to stay in lock will be briefly discussed.

The threshold condition that the loop will stay in lock in the presence of noise has been examined by a number of authors (e.g., Refs. 6, 8 and 9) and no unique solution has been obtained so far. In the presence of both interference and noise, it is noted that when the signal and interference beat heavily upon each other, the noise temporarily controls the limiter and contributes heavily to the noise output of the BPL. It is necessary that the ratio $\left[(S_S)_o - (S_I)_o\right]/N_o$ be greater than 4.5 dB [9] such that with high probability the loop will remain in lock.

For large input signal-to-noise ratio, i.e., $(S/N)_i \geq 20$ dB say, and $a^2 < 1$, the power output of the BPL due to input signal, interference and the intermodulation terms can be written as [7]

$$(S_S)_o = \frac{8}{\pi^2}\left[{}_2F_1\left(\frac{1}{2}, -\frac{1}{2}; 1; a^2\right)\right]$$

$$(S_I)_o = \frac{2a^2}{\pi^2}\left[{}_2F_1\left(\frac{1}{2}, \frac{1}{2}; 2; a^2\right)\right]^2$$

$$(S_{SI})_o = \frac{2a^2}{\pi^2}\left[{}_2F_1\left(\frac{3}{2}, -\frac{1}{2}; 2; a^2\right)\right]^2$$

$$(S_{IS})_o = \frac{1}{8\pi^2}\, a^4\left[{}_2F_1\left(\frac{3}{2}, \frac{1}{2}; 3; a^2\right)\right]^2$$

where ${}_2F_1(a, b; c; x)$ is the gaussian hypergeometric function defined by

$${}_2F_1(a, b; c; x) = \sum_{i=0}^{\infty} \frac{\Gamma(i + a)\,\Gamma(i + b)\,\Gamma(c)}{\Gamma(i + c)\,\Gamma(a)\,\Gamma(b)}\,\frac{x^i}{i!}$$

$$= 1 + \frac{ab}{c}\,\frac{x}{1!} + \frac{a(a+1)\,b(b+1)}{c(c+1)}\,\frac{x^2}{2!} + \cdots$$

and $\Gamma(\,)$ is the gamma function.

Thus

$$\left(\frac{S_I}{S_S}\right)_o = f^2 = \frac{a^2}{4}(1 + 0.375\,a^2 + 0.188\,a^4 + 0.107\,a^6 + \ldots)^2 \qquad (57a)$$

$$\left(\frac{S_{SI}}{S_S}\right)_o = g^2 = \frac{a^2}{4}(1 - 0.125\,a^2 - 0.062\,a^4 - 0.035\,a^6 + \ldots)^2 \qquad (57b)$$

$$\left(\frac{S_{IS}}{S_S}\right)_o = h^2 = \frac{a^4}{64}(1 + 0.5\,a^2 + 0.29\,a^4 + \ldots)^2 \qquad (57c)$$

Also, the output signal-to-noise ratio is related to the input signal-to-noise ratio by[7]

$$\left(\frac{S}{N}\right)_o = k(a)\left(\frac{S}{N}\right)_i$$

where k(a) is a constant depending on $\underline{a}$ only.

Setting $(S_S/N)_i = 100$, we obtain the corresponding interference-to-signal power ratio $a^2 = 0.92$. For larger input signal-to-noise ratios, the allowable a^2 would be larger for the same locking condition in the loop. The root mean-square phase error estimate for this case is computed as 0.3 rad or a peak phase error of $0.3\sqrt{2}\,(180^o/\pi) = 24.5^o$.

The above discussion has been limited to $a^2 < 1$. As $a^2 \to 1$, the intermodulation terms become more significant and the above computation appears less accurate. Therefore, for large input signal-to-noise ratios, viz. $(S/N)_i \geq 100$, it is required that the interference-to-signal power ratio at the input of the BPL should be less than 0.92 and the corresponding maximum phase error due to interference will be 24.5^o.

For medium or small signal-to-noise ratios, the BPL output powers due to signal, interference and intermodulation terms are functions of $(S_S/N)_i$. Except for large $(S/N)_i$, h is small and the estimate of phase error given by Eq. (56) takes the approximate form

$$\hat{\epsilon}_u \approx \frac{1}{\sqrt{2}} (f - g) \left[2 + (f+g)^2\right] \tag{58}$$

which is plotted in Fig. 14 as a function of $(S/N)_i$ for various values of a^2. The discrepancy between the root mean-square phase error computed from Eqs. (56) and (58) at large $(S/N)_i$ is due to the intermodulation terms. As $(S/N)_i$ decreases, the intermodulation terms fall off rapidly and Eq. (58) becomes more accurate.

For $(S_S/N)_i = 4$, the condition for the loop to remain in lock results in $a^2 = 0.4$ and the corresponding phase error estimate is obtained from Fig. 14 as $\hat{\epsilon}_u = 0.32$ rad or 26^o peak phase error.

2.3.3 Signal Suppression Factor

The effect of signal suppression in the presence of interference is denoted by a signal suppression factor α over the fundamental band defined as

$$\alpha^2 = \frac{\text{actual signal power output of BPL}}{\text{total power output of BPL}} = \frac{(S_S)_o}{(S_S)_o + (S_I)_o + (S_{SI})_o + (S_{IS})_o + \ldots + (N)_o}$$

$$\approx \frac{1}{1 + \left(\frac{S_I}{S_S}\right)_o \left[1 + \left(\frac{S_{SI}}{S_I}\right)_o\right] + \left(\frac{N}{S_S}\right)_o} \tag{59}$$

Figure 15 is a plot of the signal suppression factor vs the input signal-to-noise ratio with interference-to-signal power as a parameter. A signal-to-noise ratio 0 dB is defined as the threshold signal-to-noise ratio. The corresponding signal suppression factor α_o is denoted as the threshold signal suppression factor. When the loop operates above threshold the damping ratio, natural frequency and bandwidth of the loop are modified by the ratio α/α_o in exactly the same manner as in the no interference case, although the ratio α/α_o varies with $(S/N)_i$ differently. It is noted that the loop performs closely as a linear model when it operates above threshold.

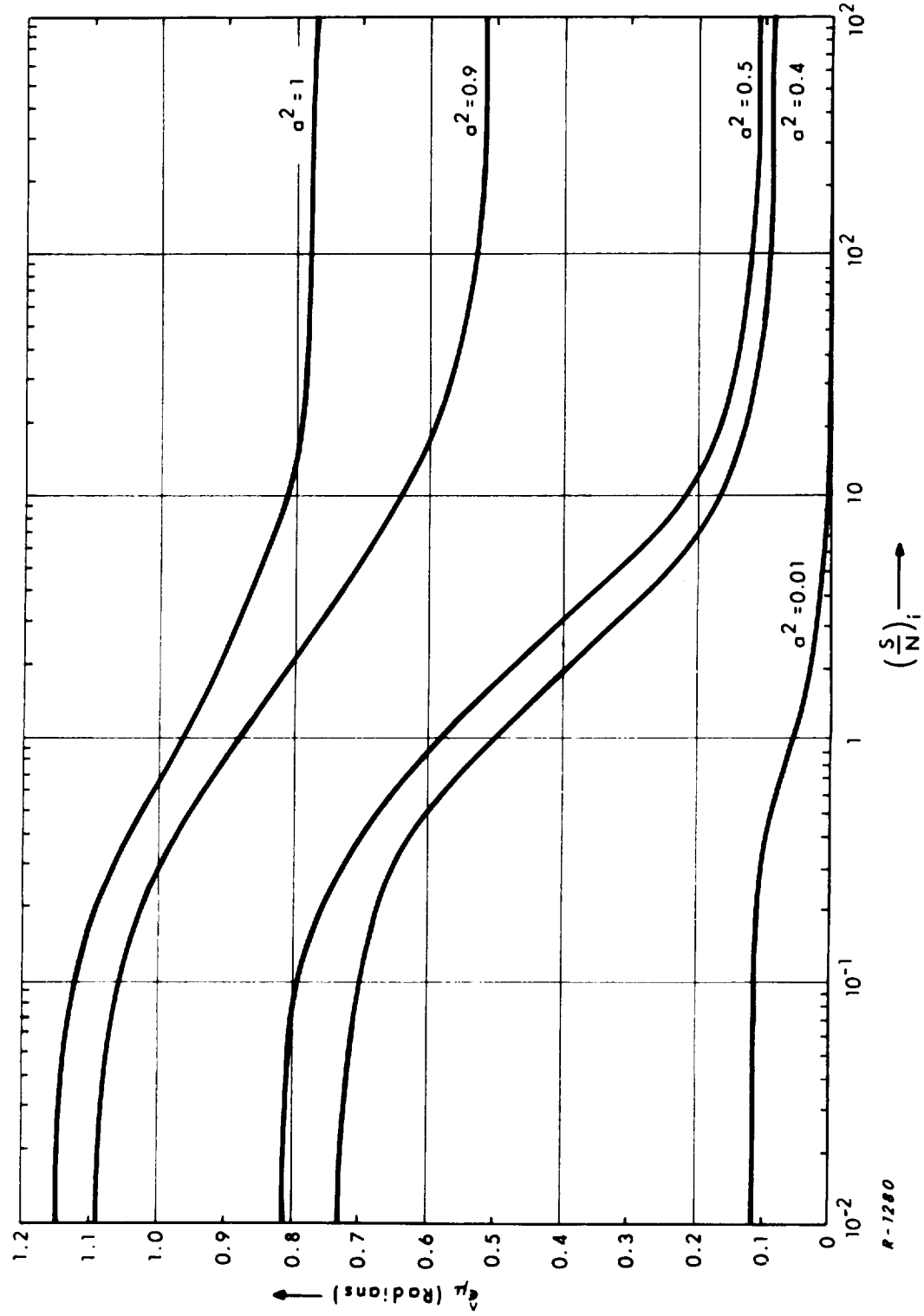

Fig. 14 Phase Error Estimate Due to Interference vs Input Signal-to-Noise Ratio.

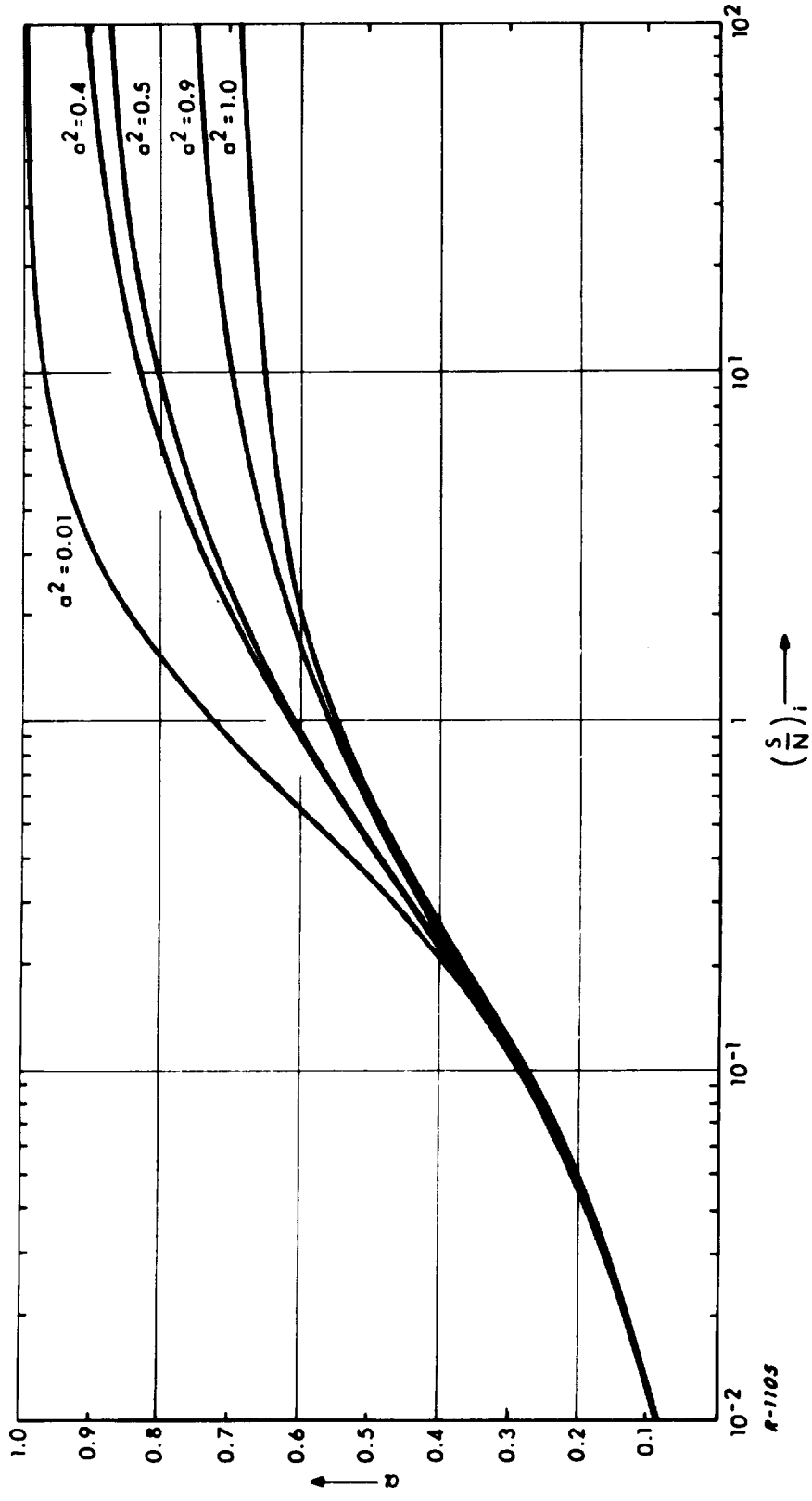

Fig. 15 Signal Suppression Factor for the BPL vs Input Signal-to-Noise Ratio.

2.3.4 Conclusion

The performance of a phase-locked loop in the presence of both interference and noise was analyzed by using the linear phase transfer model of the loop. The mean-square phase error is related to the condition for the loop to remain in lock. As expected, the interference degrades the system performance and only a small phase error is allowed; thus, the linear model is a good approximation for performance analysis. The effect of interference rejection of a bandpass limiter preceding the loop has been examined by obtaining a good estimate of root mean-square phase error and signal suppression factor. A more exact study of the loop performance in the presence of interference requires a nonlinear analysis of the loop operation.

To apply these results to the MSFN receiver and our hypothetical case of interference, we note that the two RF carriers must have very nearly equal doppler shifts to maintain the 5 Mc difference frequency so that the interfering signal will fall within the IF crystal filter and PLL passbands. The rejection of the interference will occur in two places, (1) the 50 Mc IF amplifier will filter the unwanted carrier and (2) the mixer will provide more gain to the desired output than to the second harmonic of the difference frequency. If the sum of these rejections amounts to 50 dB or more, the interference should be tolerable. This estimate is based on the exaggerated figure of "unwanted" carrier 30 dB higher than desired carrier and allowable loop input S/I ratio of 20 dB ($a^2 = 0.01$) taken as a reasonable low $(SNR)_{in}$ value from Fig. 14.

Although acquisition by the carrier loop was not analyzed here, a comment is in order. Our hypothetical interference could capture the loop during acquisition if the doppler shifts on the RF carriers were enough different that interference and signal do not both pass through the crystal filter or at least do not both fall within the loop passband. In this case no interference will occur once correct acquisition is attained.

Chapter III

PROGRAM FOR NEXT INTERVAL

1. Analyze in detail the performance of the telemetry link in the Apollo USB system considering the three different bit rates which are being implemented.

2. Study the down-voice and biomedical subcarrier link for the different signal structures being proposed for use on LEM and on CSM. Determine which of these signals gives the better performance.

3. Study the operation of the ranging system. Determine the ways in which range errors can occur and the magnitudes to be expected.

REFERENCES

1. Viterbi, A.J., "On Coded Phase-Coherent Communications," IRE Trans. on Space Electronics and Telemetry, Vol. SET-7, pp 3 - 14, March 1961.

2. Davenport, W.B., An Introduction to the Theory of Random Signals and Noise, McGraw-Hill Book Co., 1958.

3. Study, Evaluation and Analysis of Unified S-Band System for Apollo Ground Network, First Progress Report, Chapter IV, September 1964.

4. Davenport, W. B., Jr., "Signal-to-Noise Ratios in Bandpass Limiters" J. Appl. Phys., Vol.24, pp. 720-727; June 1953.

5. Jaffe, R. and Rechtin, E., "Design and Performance of Phase-Lock Circuits Capable of Near-Optimum Performance Over a Wide Range of Input Signal and Noise Levels," IRE Trans. on Information Theory. Vol. IT-1, pp. 66-76; March 1955.

6. Martin, B. D., "The Pioneer IV Lunar Probe," JPL Technical Report No. 32-215; March 1962.

7. Jones, J. J., "Hard-Limiting of Two Signals in Random Noise," IEEE Trans. on Information Theory, pp. 34-42; January 1963.

8. Sanneman, R. W. and Rowbotham, J. R., "Unlock Characteristics of the Optimum Type II Phase-Locked Loop," IEEE Trans. on Aerospace and Navigational Electronics, pp. 15-24; March 1964.

9. Second Interim Engineering Report on an Investigation of Tracking, Telemetry, and Command Systems Susceptibility to Radio Interference, Air Force Systems Command, Wright-Patterson Air Force Base, Ohio, March 1964.